THE UNIVERSITY OF MANITOBA

IMAGE RECORDING AND RECONSTRUCTION BY CURVILINEAR HOLOGRAMS

Dennis K. Morland

A THESIS

SUBMITTED TO THE FACULTY OF GRADUATE STUDIES

IN PARTIAL FULFILMENT OF THE REQUIREMENTS FOR THE DEGREE

OF MASTER OF SCIENCE

IN

ELECTRICAL ENGINEERING

WINNIPEG, MANITOBA

R3T 2N2

May, 1973

THE UNIVERSITY OF MANITOBA
ELIZABETH DAFOE LIBRARY

ABSTRACT

This thesis deals with the problem of real image formation by curvilinear holograms. A review of the pertinent literature in the field of holographic imaging is presented. An exact integral equation formulation is derived to describe real image formation by an ideal curvilinear hologram of arbitrary shape. The integral is solved exactly for the two-dimensional case. EXPERIMENT 1 examines the real image field for a point source when measures are taken to reduce the effect of physical degradation factors. Results show that the large hologram aperture and short hologram-to-object distance yields the expected limited depth-of-focus. The lack of abberrations in the image verify the advantage of using plane wave reference and reconstruction beams. EXPERIMENT 2 uses a diffusely scattering object in an arrangement similar to that of EXPERIMENT 1 in order to determine the obtainable resolution as a function of the ratio of aperture size to hologram-to-object distance. Results indicate that the obtainable resolution is about 6.8% of that of the ideal diffraction limited system. EXPERIMENT 3 shows that special precautions must be taken with curvilinear holograms in order to duplicate the resolution obtainable with planar holograms. Finally, a summary of results is presented and some comments on the practicality and applications of imaging by curvilinear holograms is made.

ACKNOWLEDGEMENTS

I wish to extend my sincere appreciation to Dr. W.M. Boerner for the guidance and encouragement he has given me in preparing this thesis.

I also wish to thank Mr. Y.M. Antar for his helpful comments.

The financial support received from the National Research Council of Canada (Grant No. A7240) and a University of Manitoba Grant in aid of research for equipment expenses is gratefully acknowledged.

In conclusion, I wish to thank Mrs. S. Clubine for her cheerful and expert typing of the manuscript.

Dennis Morland

TABLE OF CONTENTS

LIST OF FIGURES

LIST OF PHOTOGRAPHS

LIST OF SYMBOLS

Greek Alphabet:

α	Wedge angle
$\alpha, \alpha_1, \alpha_2, \alpha_3$	Generalized Fourier frequency variables
β, γ, τ	Complex variables of integration
γ	Film gamma
δ	Delta function
∇^2	Laplacian operator
θ, θ''	Polar angles
λ	Wavelength
π	Pi (3.14159...)
ρ	Radial distance of observation point
ρ'	Radial distance of source point
ρ''	Radial distance of hologram point
σ	Pole in complex γ plane
ϕ	Polar angle of observation point
ϕ'	Polar angle of source point
ϕ''	Polar angle of hologram point
ω	Angular frequency

Latin Alphabet:

a	Diameter of aperture
Å	Ångstrom unit
BS	Beam splitter

C_1, C_2	Contours of integration
d	Distance between source and observation points
D	Diffusely scattering object
E	Emulsion
F	Fringes
G	Green's function
G	Granite optical bench
h	Complex variable of integration
$H_o^{(2)}$	Zero order Hankel function of second kind
i	$[-1]^{1/2}$
J_o	Zero order Bessel function
k	Wave number $2\pi/\lambda$
K	Kernel of image response
L	Lens
LG	Liquid Gate
M	First surface mirror
$\hat{n}$	Unit normal to hologram surface
O	Object
O	60X microscope objective
P, P_i, P_s	Source function
P	XYZ Positioner
PW	Plane wave
$\bar{r}$	Observation vector
$\bar{r}'$	Source vector

$\bar{r}''$	Hologram vector
R	Hologram to object distance
r	Denotes space in which real image is found
R_o	Absorber placed at point of convergence of reconstruction source
R	Rail type optical bench
S	Source
S_h	Hologram surface
SF	40X spatial filter with 25 micron pinhole
S'	Deformed hologram surface
t	Time variable
v	Denotes space in which virtual image term propagates
V	Volume of integration
(x,y,z)	Coordinate system

chapter one

INTRODUCTION

Holography is a process wherein the phase and amplitude information of a wave diffracted from a three-dimensional object can be recorded in such a way that a duplicate or a conjugate of the original object wave can be produced at a later time. Information storage is accomplished by recording an interference pattern produced by the superposition of coherent reference and object waves. Reconstruction is done by illuminating this wave recording, the hologram, with a reconstruction beam which closely matches the original reference beam.

The basic concept of holography was originated in 1948 by Dennis Gabor as a result of his research into high resolution electron microscopy [17,18]. The inspiration for this two-step, lensless wave-reconstructing microscopy came from the invention, many years previous, of the "X-ray microscope" by Sir Lawrence Bragg [4,5]. Gabor envisioned that by recording the unfocused wavefronts themselves, the resolution limit of the electron microscope might be reduced to perhaps 1 Å, thereby making atomic structures visible. The lack of sufficiently coherent sources of X-ray and electron beams has prevented such resolution from being achieved to date. However, it should be noted that in principle holography offers a method of realizing extreme resolution, diffraction limited imaging.

The ability of holograms to store and reproduce the total information

of an object wavefront allows it to function in a virtually limitless variety of information processing and wavefront manipulation systems, many of which do not directly involve imaging [7,8,13,14,20,54,61,63]. Such applications will not be considered here; rather, the hologram will be examined solely in its role as a generator of real and virtual images of arbitrary irregular objects. Special consideration will be given to the resolution obtainable in holographically produced real images of three-dimensional objects.

Imaging properties of holograms have been conventionally treated from the viewpoint of planar hologram shapes. This configuration greatly facilitates mathematical analysis, expecially if the "paraxial approximation" is used [14,61]. In particular, Fourier transform analysis can be readily applied, thus allowing the use of the powerful techniques and theorems of Communication Systems Theory [38,54].

Investigations of such planar holograms [33,46,47,48] have yielded the fact that the resolution spot size (depth of focus) of a reconstructed real image point is inversely proportional to the effective hologram size and directly proportional to the object to hologram distance. For example, Rayleigh's criterion [71] states that diffraction limited resolution of a small circular aperture is $0.61\lambda R/a$ for a disk of diameter a at a distance R from the object, radiating at wavelength λ, where the subtended cone angle is $a/2R<<1$. Thus, a high resolution real imaging system must record a large segment of the waves diffracted from the object. A theory of curved holograms

can show that, provided "perfect" holographic recording is assumed, the resolution obtainable in the real image depends on the segment of the object wavefront that is recorded, but not on the exact hologram shape. This feature makes the topic of curvilinear holograms extremely important in the field of high resolution imaging systems.

It is the purpose of this analysis to investigate further the properties of curvilinear holograms, particularily in regard to the generation of real images.

In the literature review, a summary will be made of the pertinent contributions, both theoretical and practical, in the field of holographic imaging, with particular emphasis on curvilinear hologram shapes.

The theoretical analysis will present an integral equation description of imaging by an arbitrary curvilinear hologram modeled by a thin variable transmittance film. This analysis will be modified by consideration of the properties of real recording media as they apply to curvilinear hologram shapes.

The experimental section will describe a number of experiments to investigate properties of real image formation. Experiments 1 and 2 will serve to determine how well the resolution obtainable in a holographically produced real image compares to the resolution of an ideal diffraction limited imaging system. Results will show that the obtainable resolution, while less than the ideal, is sufficient to enable

the real image of a diffusely scattering object to be constructed with great accuracy. Experiment 3 will investigate the difficulties encountered in obtaining the real image of objects from curvilinear holograms. Results will show that in general curvilinear holograms are much more susceptible to image degrading phenomena than are planar holograms.

Finally, a summary of results will be presented and some comments on the practicality and applications of imaging by curvilinear holograms will be made.

chapter two

LITERATURE REVIEW

The principle of wave recording by the interference pattern formed by the superposition of coherent reference and object waves was first conceived by Dennis Gabor in 1948 during his research into high resolution electron beam microscopy [17,18]. He described the recording made in this way as a hologram, from the Greek word "holos", which means "whole". The science involving such wave recordings then became known as holography. Several researchers attempted to improve the obtainable resolution [13] but achieved little success. This was due to the unavailability of sufficiently coherent sources which necessitated the use of an "in line" configuration and made it impossible to effectively separate the real image, virtual image and zero order transmittance terms in the reconstruction process.

With the advent of the optical laser and the "off-axis" techniques of Leith and Upatnieks in the early 1960's [38,39,40], the various image terms could be spatially separated. Leith and Upatnieks were also the first to consider holography from the viewpoint of Communication Systems Theory [38]. These innovations made holography an important, practical engineering tool.

Holograms may be considered under three main classifications according to the manner in which they are recorded. These are: Fresnel holograms, Fraunhofer holograms and Lensless Fourier Transform Holograms [20,61,63]. In general, the Fresnel hologram is formed relatively

close to the sources where the paraxial approximation [61] cannot be used. Fraunhofer holograms are formed in the far field, and lensless Fourier Transform holograms are formed using object and reference beams with equal divergent radii so that the recording assumes many of the characteristics of Fraunhofer holograms [63] (see Fig. 1).

Although holographic recordings are often considered as a two-dimensional transmittance function (i.e. a perfectly "thin" variable transmittance film), such an assumption is good for a first approximation only and in many cases leads to completely erroneous results [8,14]. It has been shown [41,44,61] that, since photographic emulsions in particular are many wavelengths thick, holograms recorded in them must be considered as a volume diffraction grating. Analysis of such thick emulsions [13, 61,30] have shown that the conjugate image is very strongly attenuated in reconstruction. Reflection type holograms [12,13,63] can be made, due to the volume effect, by having the reference and object beams intercept in a large (nearly 180°) angle so that the fringe period approaches half a wavelength. Such volume gratings will exhibit pronounced Bragg diffraction so that, with a white light reconstruction beam, the reconstructed images will be essentially monochromatic. The bandwidth of the reflected light has been found to be approximately 50Å [13]. The spatial frequencies normally encountered in cylindrical or conical hologram shapes necessitates consideration of the volume effect.

A serious problem in holography is the inadequacy of the recording materials which results in a loss of image resolution. Silver halide

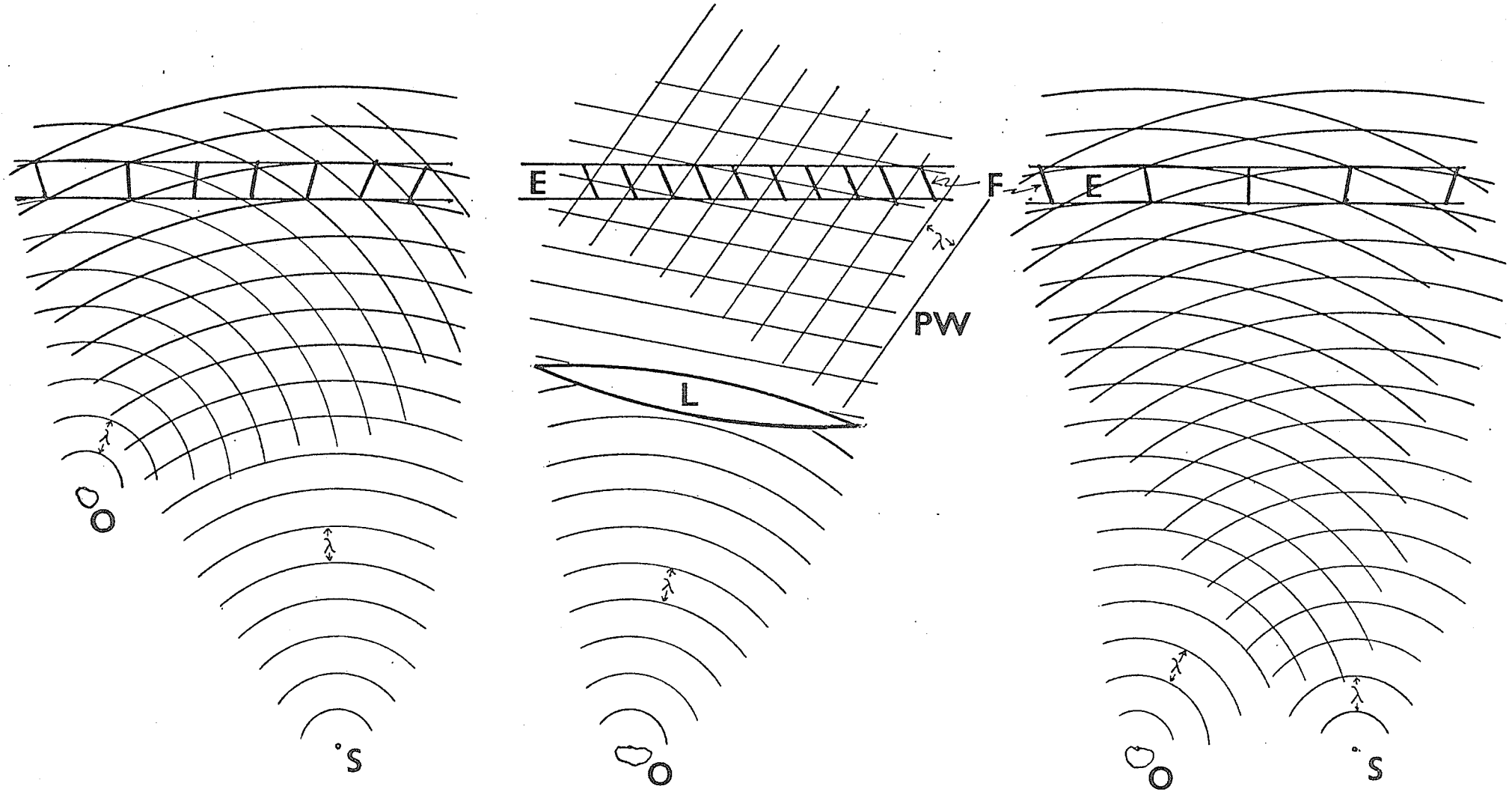

a) FRESNEL HOLOGRAM

FRINGE FREQUENCY VARIES

b) FRAUNHOFER HOLOGRAM

FRINGE FREQUENCY CONSTANT

c) LENSLESS FOURIER TRANSFORM HOLOGRAM

FRINGE FREQUENCY APPROXIMATELY CONSTANT

FIG.2.1 HOLOGRAM TYPES; (O) OBJECT, (S) POINT SOURCE, (E) EMULSION, (F) FRINGES, (L) LENS, (PW) PLANE WAVE.

recording materials are inherently noisy and resolution limited due to the finite film grain size. They are also prone to distortion due to the instability of the gelatin base. Several researchers [11,56, 34,21,43,25,13] have considered the effects of these phenomena. The nonlinearity of films [16,22,6,35,13] is another serious source of image degradation. A drawback of conventional absorption holograms is the fact that the high "bias" densities required for linear recording results in a strong attenuation of the reconstruction beam and a very low efficiency [21,61]. To overcome this problem another class of of holograms have been considered. These are "phase holograms" in which the intensity pattern is recorded as a variation in the index of refraction of a material rather than as a variation in absorptive density [61]. Latta [37] describes a method of obtaining phase holograms by chemically bleaching the processed,photographically recorded interference pattern. Others [31,13,57,9,66] experimented with a great variety of chemical bleaches. The effect of bleaching has been found to be a great increase in diffraction efficiency at the expense of image resolution and contrast [13,66]. Phase holograms have also been successfully recorded in other media including photochromic glasses [23,49], dichromated gelatins [42,58,13] and deformable thermoplastics [67,13]. These materials are very important for curvilinear holography since they offer higher resolution and less distortion than photographic films.

The possibility of object mensuration by holographic methods is an important one which has received a great deal of interest. In a series

of studies [48,47,46] Meier has shown that a holographic recording can contain sufficient information about an object scatterer to reproduce the scattering surface with a great deal of accuracy. Hildebrand and Haines [24] have proposed a method of measuring surface contours using multiple wavelengths or multiple sources. Bates [3] has experimented with constructing holograms with information gathered from X-ray analysis of objects and then regenerating the object profiles from the holograms. Mikhail [50,51] and McDonnell [45] have studied the feasibility of holographic mensuration and mapping from a photogrammetric point of view. Their technique involves manual scanning of the virtual image produced by a planar hologram to obtain the data samples. Although they have shown good accuracy with this method it has the disadvantages of being a very laborious procedure requiring highly complex instruments, subjective decision-making, and highly skilled personnel.

It is proposed that the mensuration system can be made much simpler, and perhaps automatic, if the real image is analysed instead of the virtual image. Stetson [62] used the limited-depth-of-focus effect [47,48] to generate the contour of a scattering object by intercepting the real image field from a planar hologram by another photographic film. Gara and Majkowski [19] are using a similar configuration to obtain the contours of clay models. Their system features a liquid gate to reduce film emulsion distortion and a digital sampling of the real image. Sherman [49], Wolf and Shewell [60,69] and Lalor [36] have also considered inversion of the field recorded on a planar surface.

The planar nature of most holograms permits only a limited perspective to be recorded. King [32] recorded a 360° view of an object on a planar hologram by making multiple exposures and rotating the object before each exposure. The reconstruction however still yields only a limited set of perspectives. True 360° recordings have been made by various authors [26,27,28,64,29] by surrounding the specimen by the recording film and illuminating it with a highly divergent wave. Only virtual images have been reported to date.

The images formed by such systems must be analysed by a theory of large-angle holograms to determine the increase in resolution. Mittra and Ransom [52], Wolf [68], Kozma and Zelenka [33] and Champagne [10] have considered nonparaxial imaging from large scale planar holograms. R.P. Porter [55] has shown that in curvilinear holograms, the resolution of the real image depends on subtended angle but not on aperture shape. His analysis, however, is restricted to two-dimensional holograms and further is based on the assumption of a perfect recording medium.

Clearly, a theory of three-dimensional curvilinear holograms is needed to determine the possible resolution of such a system and to predict the effect of practical limitations. It is suggested that the increased resolution and the limited depth of field obtained in a 360° hologram can be used to advantage for the purpose of object mensuration ("close-up" photogrammetry). Digitalization of the real image by a scanning photodetector may then enable the object shape to be retrieved automatically.

chapter three

ANALYSIS OF CURVILINEAR HOLOGRAMS

3.1 INTRODUCTION

The analysis is restricted to a two-step imaging process. In the first or recording step, a reference point and an object source with known radiated or scattered fields is assumed to be surrounded by a transparent recording medium of arbitrary shape. The superposition of the coherent reference and object waves produces a stable interference (intensity) pattern which is recorded by this medium. The recording is processed so that the interference pattern is represented by a variable transmittance. In the second or reconstruction step, the object and reference sources are removed and the hologram is illuminated by the conjugate of the reference wave to create a real image.

A theory of curved holograms can show that the resolution of the real image depends on the segment of the object radiation subtended by the hologram surface but not on the surface shape. An exact, integral formulation of diffraction theory is used to represent the image field produced by the hologram. The point reference hologram, whose recording arrangement is shown in Fig.3.1, is modelled by a collection of surface sources analogous to a charge and dipole layer. The surface sources can be derived from the film transmittance [55].

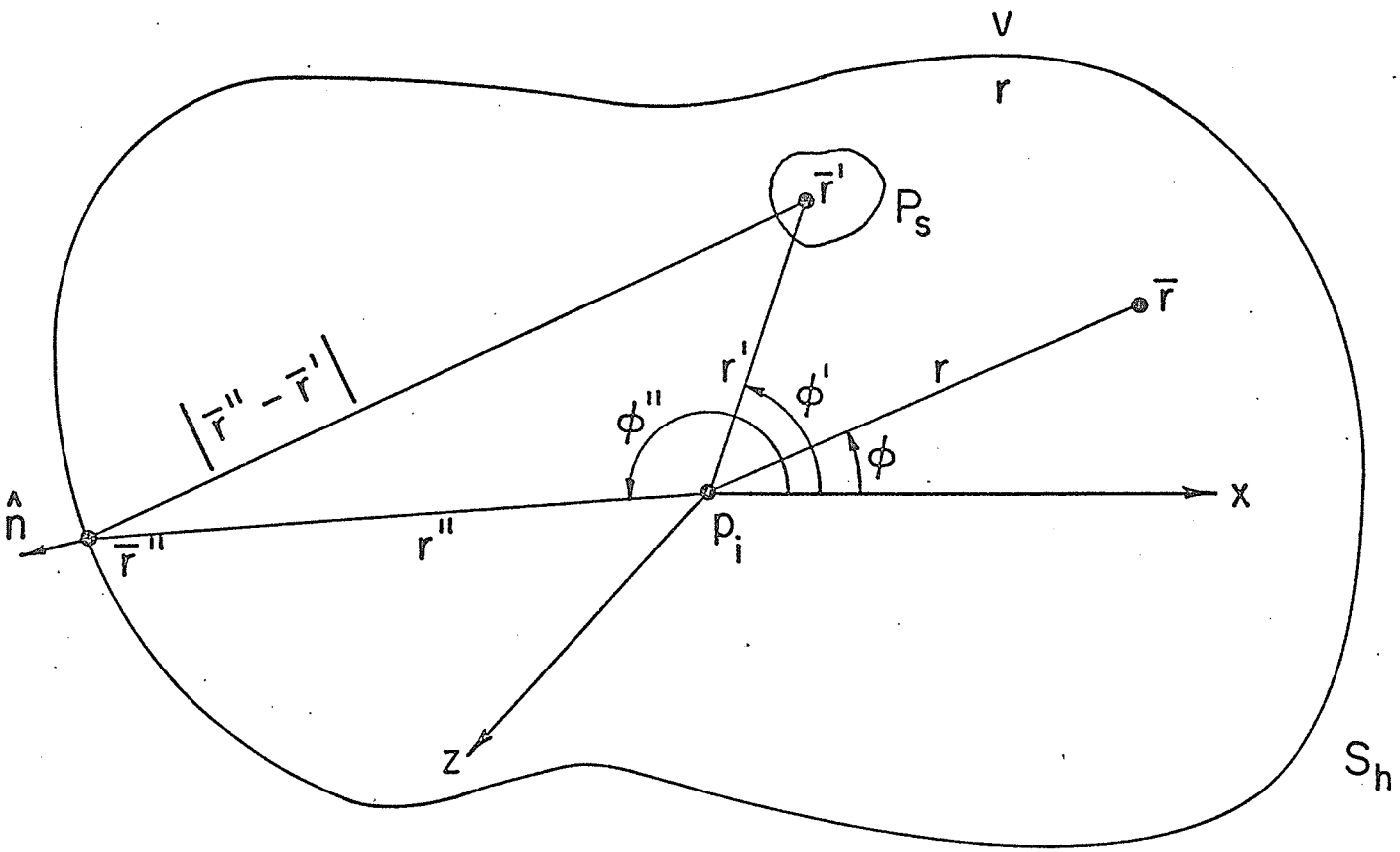

FIG. 3.1 GEOMETRY FOR A HOLOGRAPHIC SURFACE S_h OF ARBITRARY SHAPE.

Section 3.2 presents the three-dimensional Green's function formulation of diffraction theory. The basic image system is defined and analysed in Section 3.3. Section 3.4 presents the model of a point reference hologram. Section 3.5 is a brief discussion of the effects of physical characteristics of holograms on real image construction.

3.2 THREE-DIMENSIONAL GREEN'S FUNCTION FORMULATION

The theory presented here is restricted to the complex monostatic, time-independent, scalar wave equation

$$(\nabla^2 + k^2)\psi(\bar{r}) = -p(\bar{r}) \quad , \tag{1}$$

where k is the wavenumber $2\pi/\lambda$ and λ is the wavelength of the radiation.

For the time dependence $\exp(i\omega t)$ and a lossless, isotropic medium, the scalar Green's function [71] that satisfies

$$(\nabla^2 + k^2)G(\bar{r},\bar{r}') = -\delta(\bar{r} - \bar{r}') \quad , \tag{2}$$

is

$$G(\bar{r},\bar{r}') = \frac{\exp(-ik|\bar{r} - \bar{r}'|)}{4\pi|\bar{r} - \bar{r}'|} \quad , \tag{3}$$

where $\bar{r}'$ denotes the source coordinates and $\bar{r}$ denotes the observation coordinates. If the response to a finite source $p(\bar{r})$ satisfies the Sommerfeld radiation condition and is unique and linear[75], the field due to a collection of such sources is

$$\psi(\bar{r}) = \int_V p(\bar{r}')G(\bar{r},\bar{r}')dV' \quad , \tag{4}$$

where the integral is over the volume V that contains all the sources. The basic image system and the transmission hologram can be defined by

specifying the field difference across the hologram. With reference to Fig.3.1, the surface sources are related to the discontinuities in the field by the relations

$$\psi_r(\bar{r}'') - \psi_v(\bar{r}'') = \sigma_1 \quad , \tag{5}$$

$$\hat{n}\cdot[\nabla''\psi_r(\bar{r}'') - \nabla''\psi_r(\bar{r}'')] = \sigma_o \quad , \tag{6}$$

where ψ_r and ψ_v are evaluated in the r and v spaces of Fig.3.1 and where ∇'' is the gradient in $\bar{r}''$ coordinates. Equations (5) and (6) are the boundary conditions, given by Maue [74], for the scalar wave equation and σ_o and σ_1 are zero and first order surface singularity sources respectively. These surface sources can be used to find the field on either side of an arbitrary surface S_h by substituting the sources into Eqn.(4) and then performing the integration across the surface in the direction of its unit normal $\hat{n}$ [74].

The field is

$$\psi(\bar{r}) = \left\{ \begin{array}{ll} \psi_r(\bar{r}) & \bar{r} \text{ in r space} \\ \psi_v(\bar{r}) & \bar{r} \text{ in v space} \end{array} \right\}$$

$$= \int_{S_h} \{\sigma_o G(\bar{r},\bar{r}'') - \sigma_1 \hat{n}\cdot\nabla'' G(\bar{r},\bar{r}'')\} dS''. \tag{7}$$

3.3 BASIC IMAGE SYSTEM

The basic image system, as defined by Porter [55], is the collection of zero and first order sources on a surface, surrounding the location of the object during the first step, that form an image of a point object by launching a converging spherical wave during the second step. With reference to Fig.3.1, the converging wave is launched

from the hologram surface S_h and forms a real image in the r space, inside S_h. This image forming wave then diverges and passes out of the hologram surface into the v space, outside S_h (Fig.3.1). The image forming field of a point source, the point response of the system, is called the kernel and is denoted by K.

The image kernel for an arbitrary hologram surface S_h can be determined from Eqn.(7). The appropriate zero and first order sources, $\hat{n}\cdot\nabla''G^*(\bar{r}'',\bar{r}')$ and $G^*(\bar{r}'',\bar{r}')$, are found by substituting the appropriate Green's function into Eqn.(5) and Eqn.(6). The real image kernel has been found by Porter [55] to be

$$K_r(\bar{r},\bar{r}') = \int_{S_h} \{G(\bar{r},\bar{r}'')\nabla''G^*(\bar{r}'',\bar{r}') - G^*(\bar{r}'',\bar{r}')\nabla''G(\bar{r},\bar{r}'')\}\cdot\hat{n}dS'' \quad (8)$$

Following Eqn.(4), the real image field can be written in terms of this kernel as

$$\psi_r(\bar{r}) = \int_V p^*(\bar{r}')K_r(\bar{r},\bar{r}')dV' \quad (9)$$

by the principle of superposition.

Since S_h will be considered here to be in general a cylindrical shape, the three-dimensional Green's function will be represented in a more appropriate form. As shown in *appendix* A.1, the Green's function can be written as

$$\frac{\exp(-ik|\bar{r} - \bar{r}'|)}{4\pi\ \bar{r} - \bar{r}')} =$$

$$= \frac{-i}{8\pi}\int_{-\infty}^{\infty} H_o^{(2)}([\rho^2+\rho'^2-2\rho\rho'\cos(\phi-\phi')]^{1/2}[k^2-h^2]^{1/2})\exp(ih|Z-Z'|)dh \quad , \quad (10)$$

where we have used

$$|\bar{r} - \bar{r}'| = [\rho^2+\rho'^2-2\rho\rho'\cos(\phi-\phi') + (Z-Z')^2]^{1/2} \quad . \quad (11)$$

We may now consider the case where the hologram surface S_h only partly surrounds the object. With reference to Fig.3.2, consider a hologram surface that is asymptotic to a wedge of angle α at infinity. For $\bar{r}$ and $\bar{r}'$ to the right of S_h in Fig.3.2, the divergence theorem can be used to show

$$\int_{S_h} \{\quad\} \cdot \hat{n}dS'' = \int_{S'} \{\quad\} \cdot \hat{n}dS'' \quad , \quad (12)$$

where the integrand is that of Eqn. (8).

The integration can be simplified if S' is deformed to an arc of a circle of radius ρ'' centered at the object point, since in this case the unit normal to the surface S' has a radial component only. For large ρ'' , we can use the approximation to the zero order Hankel function of the second kind

$$H_o^{(2)}(\beta\rho'') = [\frac{2}{\pi\beta\rho''}]^{1/2}\exp(-i(\beta\rho'' - \pi/4)) \quad , \quad (13)$$

$$\rho'' \to \infty$$

where $\beta^2 = k^2 - h^2$.

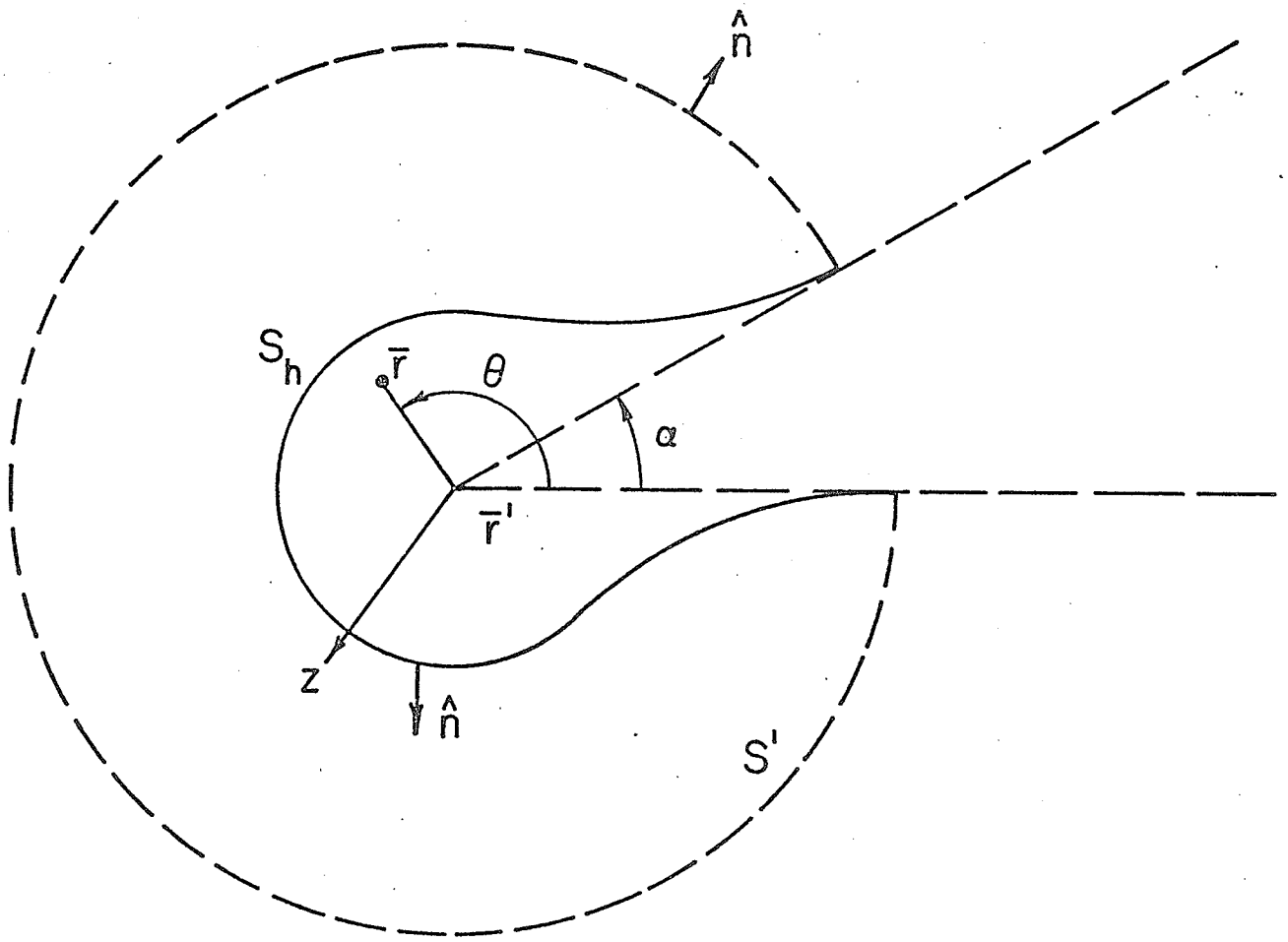

FIG. 3.2 GEOMETRY FOR OPEN HOLOGRAM ASYMPTOTIC TO WEDGE OF ANGLE α.

Defining $d = |\rho - \rho'|$ and using the approximation to the cosine law $|\rho - \rho''| = [\rho'' - d\cos(\theta'' - \theta)]$, see Fig.3.2, we can write the kernel in the r space as

$$K_r(\bar{r},\bar{r}') \cong \frac{i}{16\pi} \int_{S'} \Big[\{\beta^{-1/2}\exp(-i\beta[\rho''-d\cos(\theta''-\theta)])\exp(ih|Z-Z''|)dh\}$$

$$\times \{\int_{-\infty}^{\infty} \beta^{+1/2}\exp(i\beta\rho'')\exp(-ih|Z''-Z'|dh\}$$

$$-\{\int_{-\infty}^{\infty} \beta^{-1/2}\exp(i\beta\rho'')\exp(-ih|Z''-Z'|dh\} \quad \times$$

$$\{\int_{-\infty}^{\infty} \beta^{1/2}\exp(-i\beta(\rho''-d\cos(\theta''-\theta)))\exp(ih|Z-Z''|)dh\}\Big]d\rho''d\theta''dZ'' \qquad (14)$$

As Sherman [59] has noted in similar problems, it is very difficult to evaluate such integrals to find the image kernel. However, since we are primarily interested here in finding the resolution as a function of the angle α, we can easily solve the equation for the two-dimensional (ρ,ϕ) case to find the kernel in the r space as

$$K_r(\bar{r},\bar{r}') = \frac{i}{4\pi} \int_{\alpha}^{2\pi} \exp[jkd\cos(\theta'' - \theta)]d\theta'' \,. \qquad (15)$$

The kernel depends only upon the wedge angle α and not on the exact shape of S_h. When $\alpha = o$, the kernel becomes

$$K_r(\bar{r},\bar{r}') = \frac{i}{2} J_o(kd) \,. \qquad (16)$$

3.4 MODEL OF POINT REFERENCE CYLINDRICAL HOLOGRAM OF INFINITE EXTENT

Consider Fig.3.1 with the coordinate system centered on the reference source located at R_o, with $\bar{r}''$ the variable distance from the film to the point source. The total radiated field on the film is

$$\psi_o(\bar{r}'') = \psi_S + \exp(-ik\bar{r}'') \; / \; 4\pi\bar{r}'' \tag{17}$$

where ψ_S is the field radiated from the object source P_S. The recording medium is sensitive to the irradiance

$$I = \frac{1}{2}\,\psi_o\psi_o^* \quad , \tag{18}$$

which is the time average of the square of the field [71]. If we assume that the object field is very much less than the reference field, we can write

$$I \cong \frac{1}{2}\left[\frac{1}{(4\pi\bar{r}'')^2} + \frac{\psi_S^*\exp(-ik\bar{r}'')}{4\pi\bar{r}''} + \frac{\psi_S\exp(ik\bar{r}'')}{4\pi\bar{r}''}\right]. \tag{19}$$

If this intensity pattern is recorded by a photographic emulsion, the processed film can be described, to a first approximation, by a transmittance $T \cong AI^{\gamma}$ [14,61]. Here, γ is the developing exponent, assumed to be one, and A is a film-exposure coefficient that can vary from point to point along the film.

The reference field is reconstructed when the film-exposure coefficient is

$$A \propto 2(4\pi\bar{r}'')^2 \tag{20}$$

Without loss of generality, the proportionality constant will be taken as one.

Therefore the transmittance is

$$T = 1 + 4\pi\bar{r}'' \left[\psi_S \exp(ik\bar{r}'') + \psi_S^* \exp(-ik\bar{r}'')\right]. \tag{21}$$

To form the real image, the film must be illuminated from the outside by a converging wave $\exp(ik\bar{r}'')/4\pi\bar{r}''$. The field in the r space of Fig.3.1 during reconstruction then becomes as shown in Fig.3.3

$$\psi = T \frac{\exp(ik\bar{r}'')}{4\pi\bar{r}''} \tag{22}$$

$$= \frac{\exp(ik\bar{r}'')}{4\pi\bar{r}''} + \psi_S^* + \psi_S \exp(2ik\bar{r}'') + \psi' \,, \tag{23}$$

where ψ_S^* is the converging real image field and ψ' is the field diverging from the real image. The first and third terms in Eqn.(23) will be spatially separated from the image term if $\bar{r}'$ has a sufficiently large Z' component [61]. That is, they will be separated if the object and source points are widely separated on the Z-axis.

The resolution obtainable in the ideal case of a cylindrical hologram of infinite extent can be determined if we let the field ψ_S be the radiation from a point object at $\bar{r}'$, the free space Green's function [71], given in Eqn.(3). The converging wave must then be the complex conjugate of this function, $G^*(\bar{r},\bar{r}')$. For a point object at $\bar{r}'$, the real image field will be

$$\psi_r = G^*(\bar{r},\bar{r}') + \psi' \,, \tag{24}$$

where ψ' is the field diverging from the image. Since ψ_r must

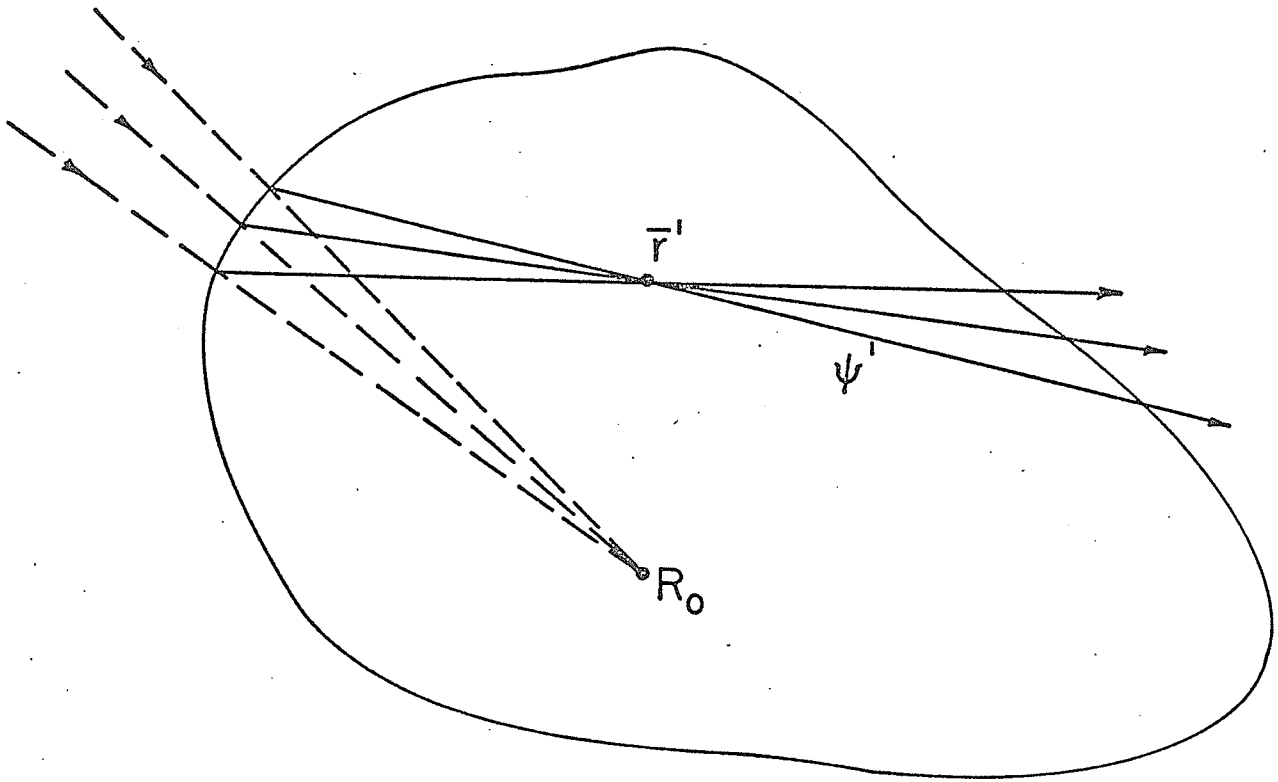

FIG. 3.3 HOLOGRAM ILLUMINATED BY RECONSTRUCTION SOURCE AND BY THE FIELD ψ' DIVERGING FROM THE IMAGE AT $\bar{r}'$

satisfy the homogeneous scalar wave equation (i.e.Eqn.(1) with the source equal to zero), then we find that

$$(\nabla^2 + k^2)\psi'(\bar{r},\bar{r}') = \delta(\bar{r} - \bar{r}'). \tag{25}$$

From Eqn.(2) it is obvious that $\psi' = -G(\bar{r},\bar{r}')$. Therefore the image field in the r space is

$$\psi_r = G^*(\bar{r},\bar{r}') - G(\bar{r},\bar{r}') \quad . \tag{26}$$

Substituting Eqn.(3) into Eqn.(26) yields the result

$$\psi_r = \frac{i}{2\pi} \frac{\sin(k|\bar{r}-\bar{r}'|)}{|\bar{r}-\bar{r}'|} \quad . \tag{27}$$

This function represents an impulse at the point $\bar{r}'$. According to the Rayleigh criterion [71], the resolution, and hence the depth of focus, is equal to twice the distance between the maximum and the first minimum of Eqn.(27), which is $\lambda/2$. Since the volume of the image point in Eqn.(27) does not change as a function of $\bar{r}'$, then the system is an ideal isoplanatic one.

3.5 DISCUSSION

As demonstrated in the above analysis, the theoretical maximum resolution of a large-extent cylindrical holography system is on the order of the wavelength of the light involved. In any real system many sources of distortion of the wavefronts (to be listed in *chapter four*) will combine to reduce the available resolution by a large amount. However, the resolution of the system could be decreased by a hundred-

fold and still provide very accurate imaging of three-dimensional objects. In order to make the preceding analysis useful in the consideration of real curvilinear holographic systems, experiments must be performed which relate theoretical resolution to the resolutions obtainable in real holographic systems with typical amounts of distortion.

In the experimental section which follows, experiments will be described which demonstrate the depth-of-focus, aberrations and resolution of typical holographic imaging systems. EXPERIMENT 1 demonstrates that the expected aberration-free and limited depth-of-focus point image can be obtained in a holographic real image. EXPERIMENT 2 verifies that the resolutions in the holographic real image is a function of the effective aperture size. The results of these experiments can be used in conjunction with the preceding theoretical model to predict the performance of real curvilinear hologram imaging systems.

Eqn.(15) indicates that the maximum resolution of a real image point in a constant Z plane depends upon the segment of the point radiation that the hologram originally subtended. For a diffusely scattering object of complicated shape, the amount of hologram surface that a given object surface element will illuminate depends upon the neighboring surface. For example, an element at the bottom of a concave hollow will illuminate less area than an element at the top of a convex bump. Hence, the resolution of a reconstructed surface element will vary considerably for different object points. As a final note, it should be noted that planar holograms can be considered as curvilinear holograms that subtend only a small segment of object radiation.

chapter four

EXPERIMENTS

4.1 INTRODUCTION

In the preceeding section an analysis has been presented which indicates that the maximum resolution of a holographically-produced real image point is on the order of the wavelength of the light used. The resolution was found to be a function of the solid angle of the object radiation that the hologram surface subtends. Such extreme resolution is the absolute limit that a "perfect" system can achieve. Hence, any physical imaging system will always exhibit lesser resolution. In particular, degradation of holographically produced images may result due to any one or a combination of the following phenomena: insufficient coherency of interfering illumination [14], shifts in the interference pattern during recording due to vibration, air turbulance or heat gradients [13,14], distortion of recording media (for example, shrinkage of film emulsion during processing) [13], inherent limitations of the recording media (for films; resolution limits and film grain noise) [20,61], non-linear recordings [22,35], and the inability to duplicate exactly (or generate the conjugate of) a reference beam [20,63].

Judicious choice of apparatus and careful design of the holographic experiment can reduce but never totally eliminate these degradation factors. So the question remains as to whether curvilinear holograms can be used to create real images with a high degree of resolution in a holographic

laboratory of modest resources. This is akin to the question of whether the technique is feasible for practical applications.

As part of a feasibility study, the following experiments were conducted.

4.2 EXPERIMENT 1 : Imaging of a Point Source

The purpose of this experiment was to investigate the ability of a hologram to produce the real image of a point source when the effective hologram area is large compared to the hologram-to-object-point distance. The experiment was designed to eliminate as much as possible the physical degradation effects referred to previously. With reference to Fig. 4.1 and Photo. 4.1, the experimental arrangement possesses the following features:

1) The difference between the path lengths of the object and reference beams is very much less than the coherent length of the laser source. This is necessary to achieve maximum contrast of the interference fringes.
2) A stable interference pattern during recording is ensured by using well designed optical components, a short exposure time, and a massive granite optical table mounted on pneumatic tires to reduce vibration.
3) The recording medium is Kodak 649F film plate.* This is an extremely high resolution emulsion with a glass plate backing for stability [72].

---

* see *Appendix* A.2 for Processing Procedure

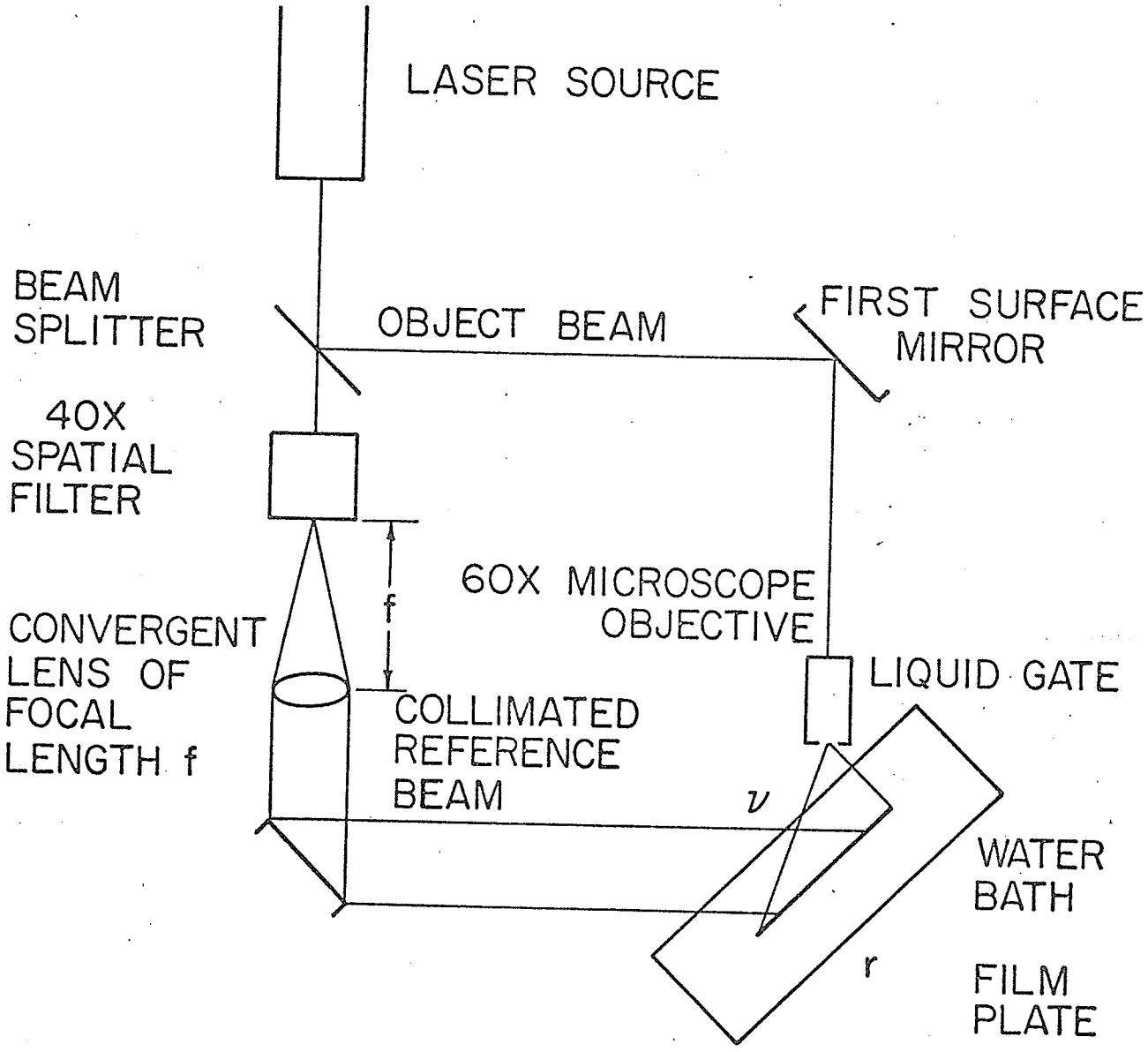

FIG. 4.1 ARRANGEMENT FOR POINT SOURCE IMAGING

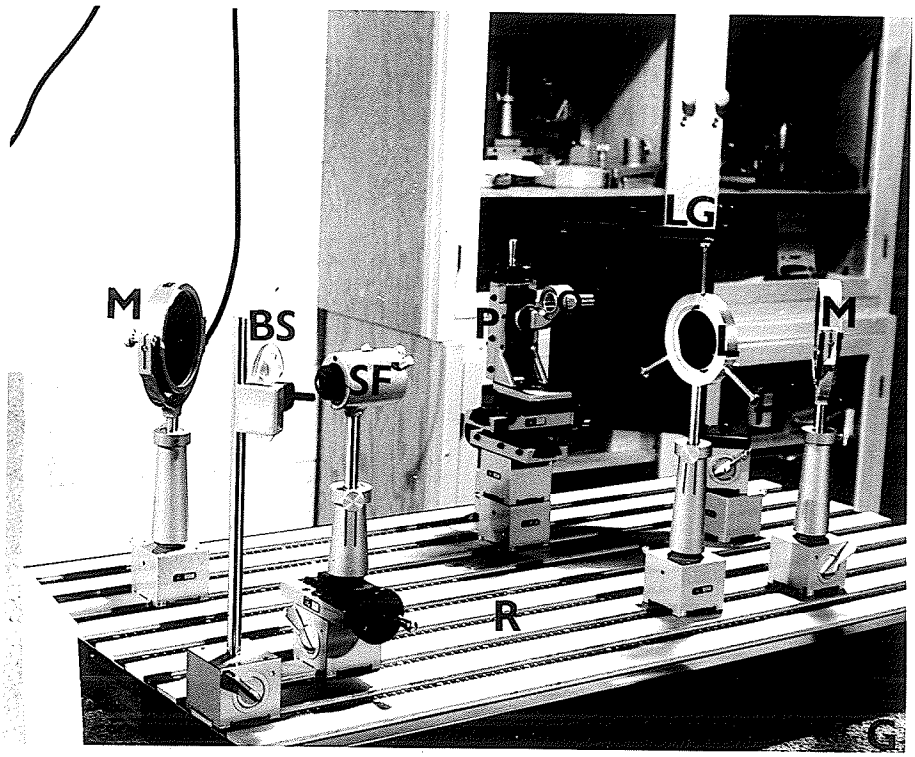

Photograph 4.1 Arrangement for point source imaging. The arrangement is shown schematically in Fig.4.1. The equipment is identified as follows: (BS) beam splitter, (SF) 40X spatial filter with 25 micron pinhole, (L) well corrected converging lens, (M) first surface mirror, (G) granite optical bench, (R) rail type optical bench, (P) XYZ positioner, (O) 60X microscope objective, (LG) liquid gate containing film plate in a water bath. To the left of this photo but not seen is a Spectra Physics model 124A HeNe laser.

4) An extremely small object point is produced by passing the collimated laser beam through a 60X microscope objective ($\frac{\text{laser beam diameter}}{60}$ = .018mm).

5) A collimated reference wave of 7.6 cm. diameter is produced by positioning a well-corrected lens a focal length away from the point aperture of a spatial filter. By using a highly diverging (40X) lens in the spatial filter, the amplitude of the reference wave is made approximately constant across its diameter. A collimated reference beam also has the advantages that the conjugate to a plane wave is simply another plane wave travelling in the opposite direction, and, the fringe frequencies in the hologram are restricted which results in a decreased influence of the film modulation transfer function.

6) The axes of both sources are oriented at 45° to the film plate so that the interference fringes formed in the photographic emulsion lie roughly perpendicular to the film surface. This greatly decreases the distortion of the fringes caused by the emulsion shrinkage during photographic processing.

7) In order to minimize the effect of surface roughness of the emulsion, the film is immersed in a water bath in a "liquid gate" film holder. The water acts as an index of refraction matching solution.

8) A linear recording of the interference pattern is achieved by using a large reference beam to object beam ratio and by biasing the exposure at approximately the half transmittance point.

9) Chemical bleaching of the hologram was not done for although bleaching increases the efficiency of the reconstruction, it also

increases the scattering noise of the emulsion.

After the film plate is exposed, it is processed according to the procedure outlined in *appendix* A.2. The processed hologram is then replaced in the liquid gate holder in a reversed position from that of recording. This effectively introduces the reconstruction illumination as a conjugate of the reference beam. The real image is formed (Fig.4.1) in the "r" space and can be recorded on film. The depth of focus and the spot size of the focused point is determined by orienting a flat film perpendicular to the axis of convergence of the spot and then making several exposures along this axis.

The use of a point source allows the observer to gain considerable information on the performance of the imaging system. For instance, the depth of focus can be found very readily. Also, aberrations such as astigmatism and spherical aberration [61] can be identified from the real image field.

Results: The results of this experiment are shown in Photographs 4.2, 4.3 and 4.4. The depth of focus is seen to be extremely limited and the size of the focused image point is comparable with the original point. Furthermore, the image does not exhibit noticable amounts of spherical aberration, astigmatism or coma aberration.

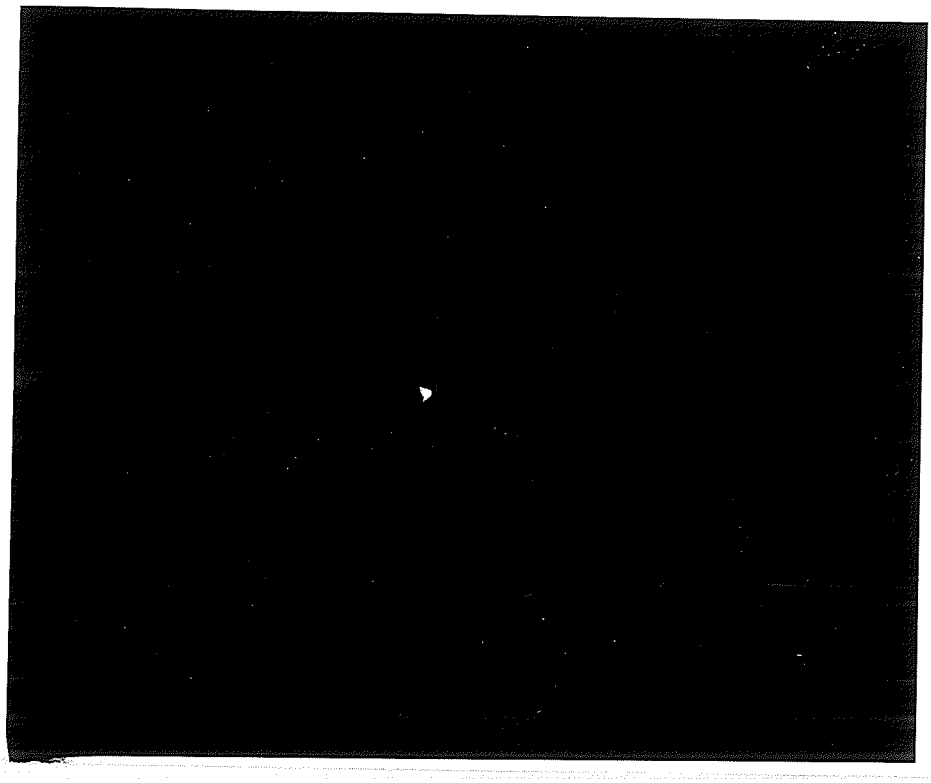

Photograph 4.2 Point reconstruction; in focal plane (enlarged)

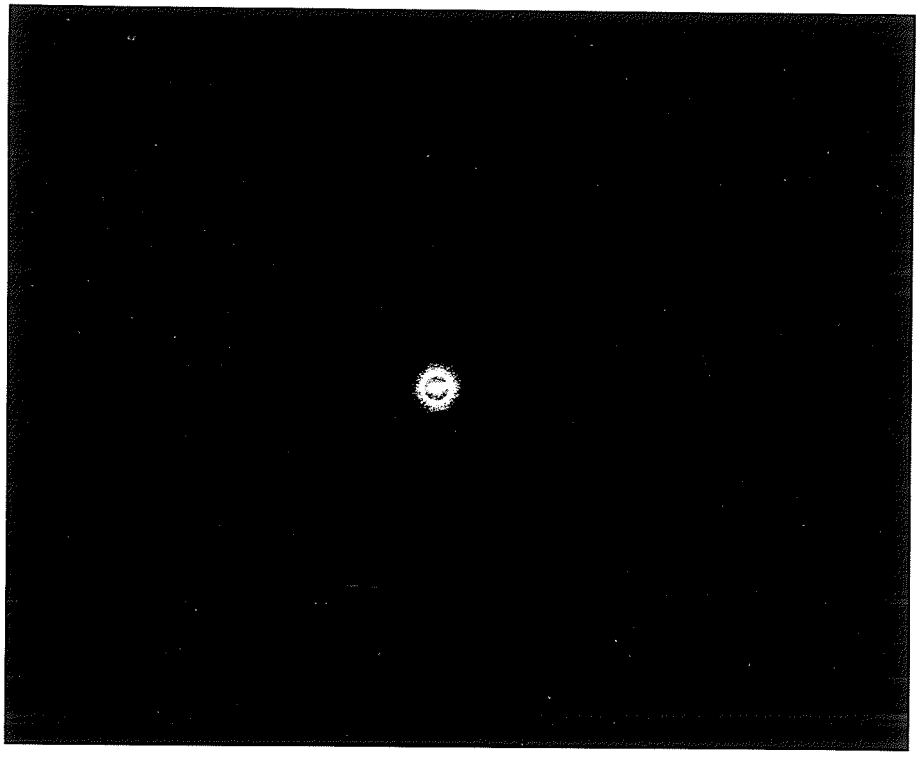

Photograph 4.3 Point reconstruction;
.79mm from focal plane
(enlarged)

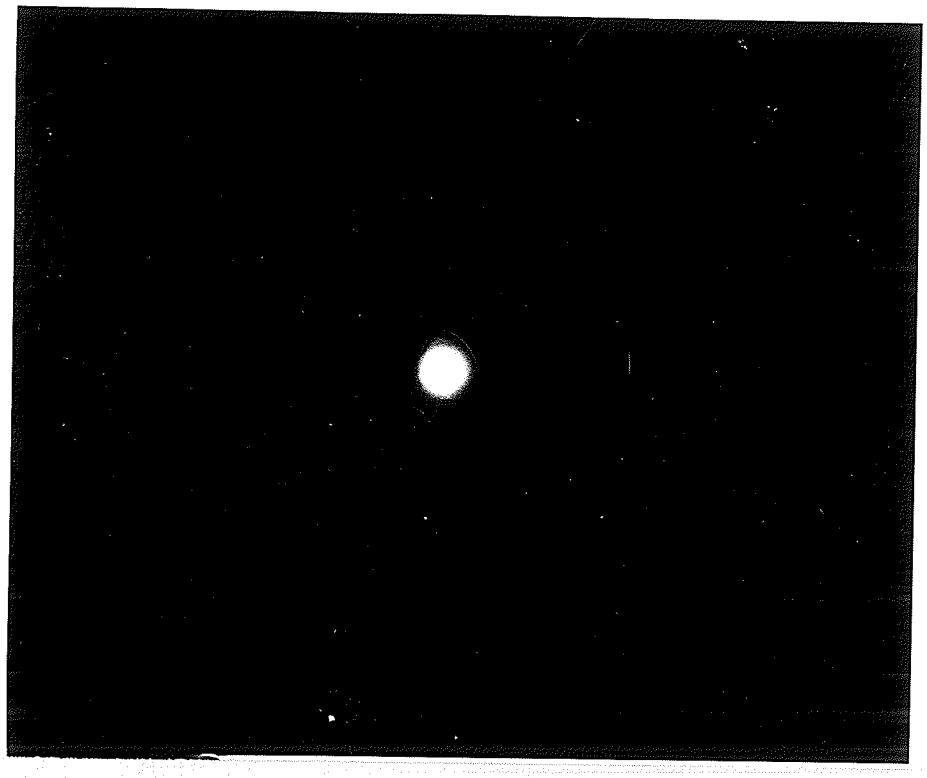

Photograph 4.4 Point reconstruction;
1.58mm from focal plane
(enlarged)

4.3 EXPERIMENT 2 : Imaging of a Diffusely Scattering Object

The purpose of this experiment was to investigate the ability of a hologram to produce the real image of a diffusely scattering object when the effective hologram area is large compared to the hologram-to object distance. With reference to Photo. 4.5, this experiment is very similar in nature to the preceeding one, with the exception that a diffusely scattering object is used instead of a point source. The real image is produced and sampled in a similar way.

The object is a standard resolution test chart illuminated with highly diffuse light. The test chart consists of five sets of equally spaced bright and dark lines. Each set is half the size of the preceeding one. Such a chart is highly useful in determining the performance of an imaging system since the frequency (in line pairs per millimeter) of the finest set of resolvable lines in the image is the resolving power of the system. The resolution spot size of the system may then be taken as the reciprocal of this frequency.

Results: The results of this experiment are shown in Photographs 4.6, 4.7 and 4.8. It is seen that the finest set of lines on the test chart is resolvable. This means that the resolution of this system is equal to or greater than 19 line pairs per millimeter. This corresponds to a spot size of about .053 millimeter.

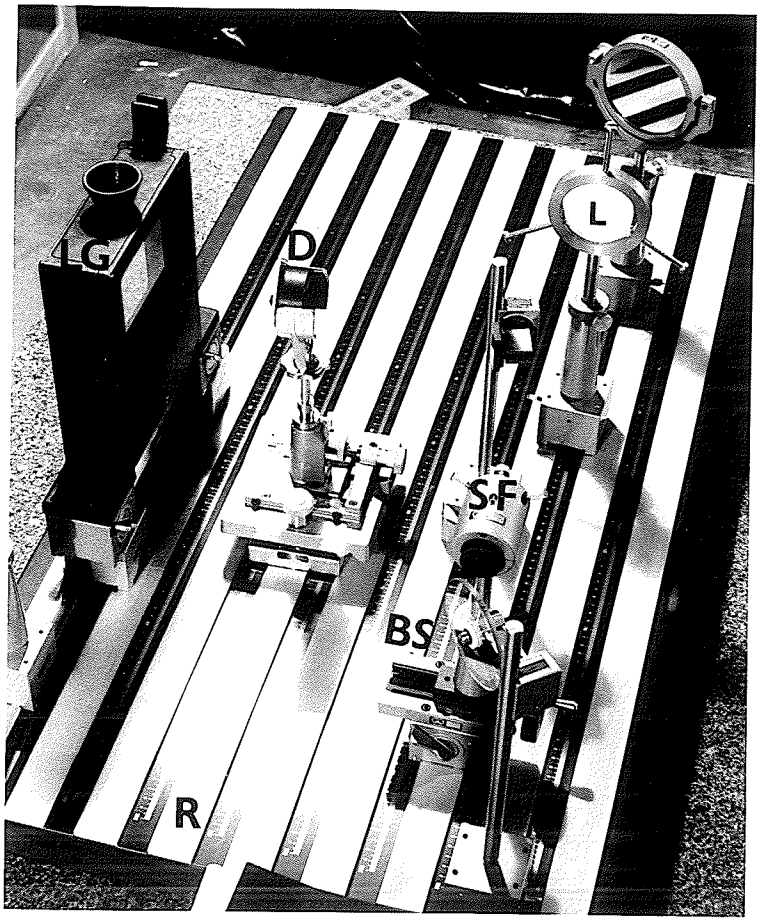

Photograph 4.5 Arrangement for diffuse scatterer (D) is the diffusely scattering resolution chart. Other equipment is identified by caption of Photograph 4.1

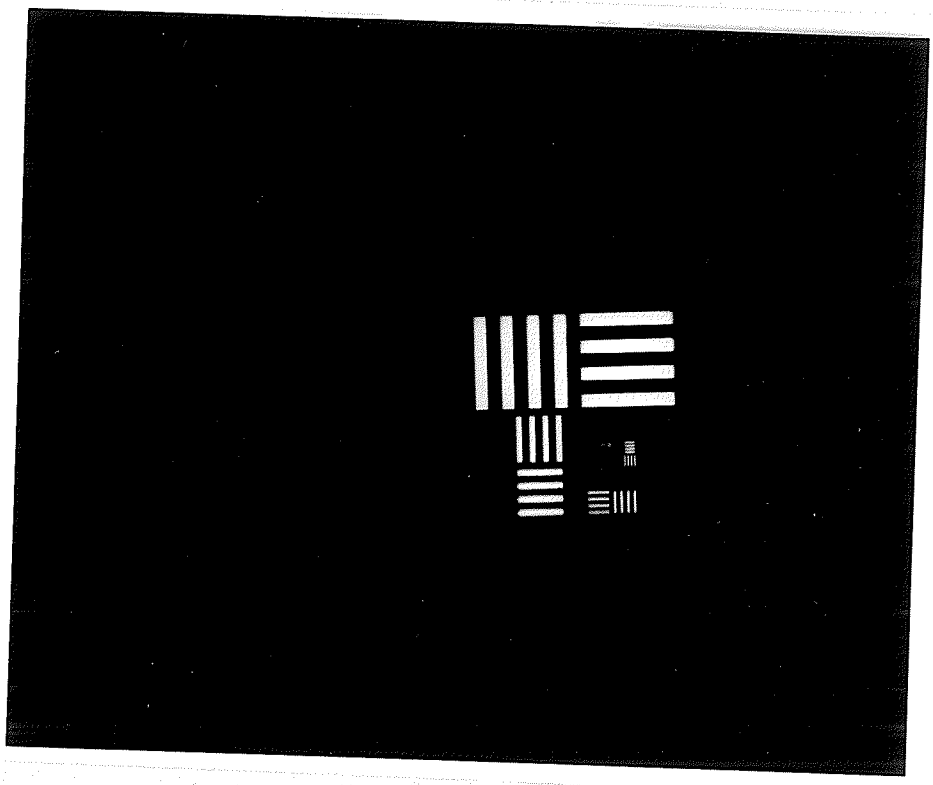

Photograph 4.6 Reconstruction of resolution pattern; in focal plane

(enlarged)

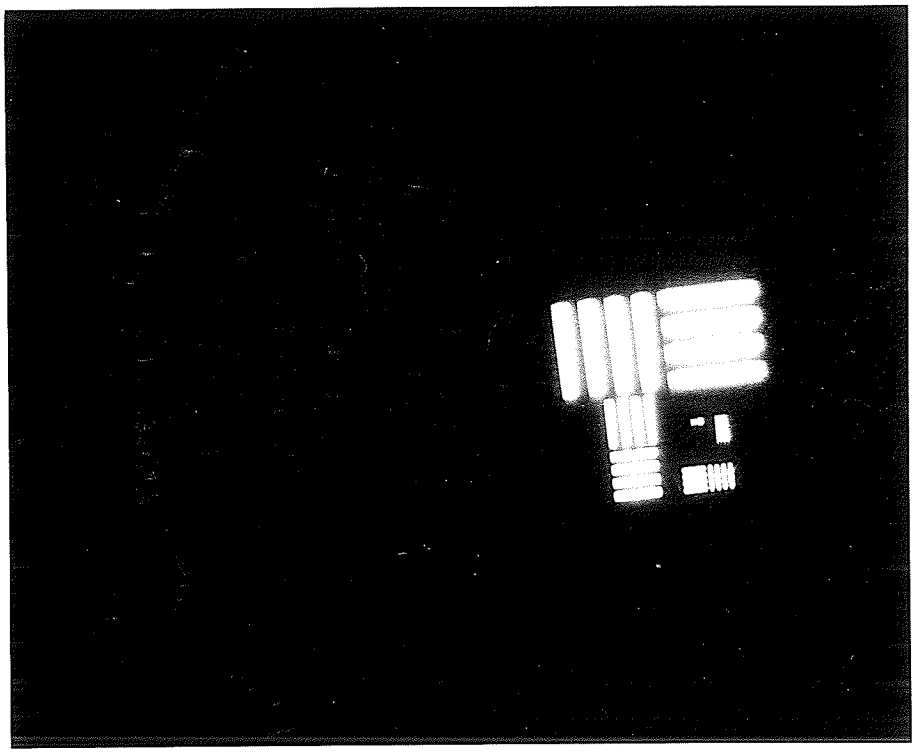

Photograph 4.7 Reconstruction of resolution pattern; .5mm from focal plane (enlarged)

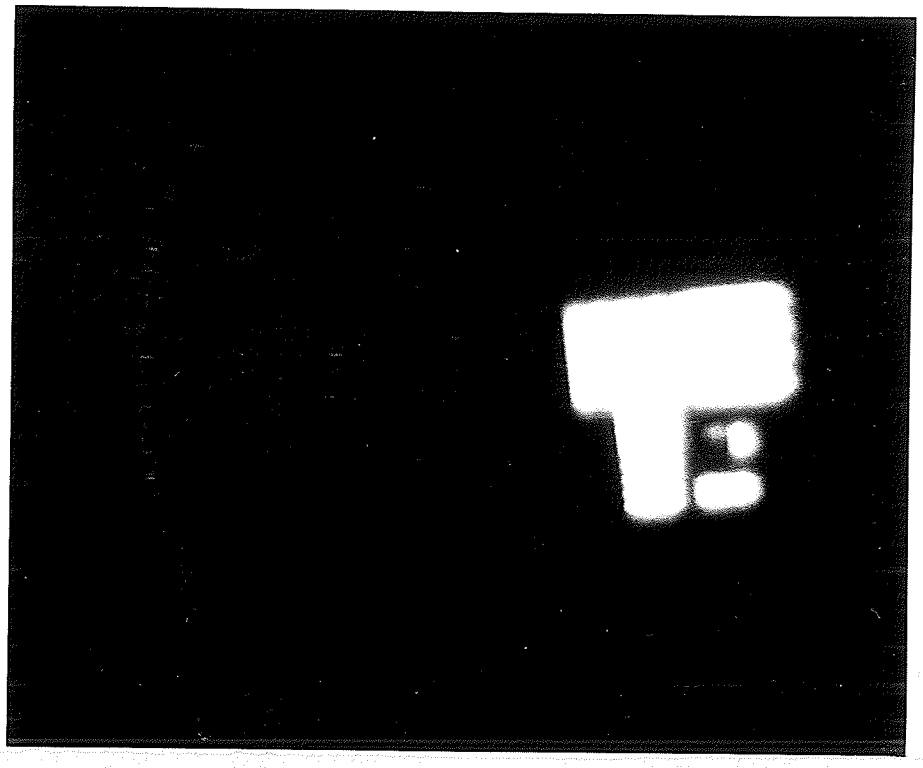

Photograph 4.8 Reconstruction of resolution pattern; 1mm from focal plane

(enlarged)

4.4 EXPERIMENT 3 : Circular Cylindrical Holograms

The purpose of this experiment was to investigate the difficulties encountered in generating the real image from 360° holograms using conventional techniques. Since a curvilinear hologram was required, a flexible film had to be used; in this case, Agfa-Gaevert 10E75 4x5 inch sheet film [1,15,70]. Flexible film provides much less dimensional stability than glass plates, hence, some distortion of the fringes in the emulsion is inevitable. Since a liquid gate to accommodate curvilinear films was not available, the effect of surface roughness of the emulsion could not be eliminated and posed a serious deleterious effect on image formation. The fringe planes in curvilinear holography cannot be constrained to lie roughly perpendicular to the emulsion surface over much of the surface area, hence, considerable distortion results when the emulsion shrinks during photographic processing. In cylindrical holography it is extremely difficult to produce a satisfactory conjugate reference beam due to the flexible nature of the film and simply the lack of suitable optics to produce a large scale converging wave. As a consequence, only virtual images have been produced to date when a spherical reference wave has been used.

Fig. 4.2 illustrates the holographic method and Photo. 4.9 shows a typical virtual image.

Results: A number of cylindrical holograms have been made using the arrangement of Fig. 4.2. In general, the virtual images produced by

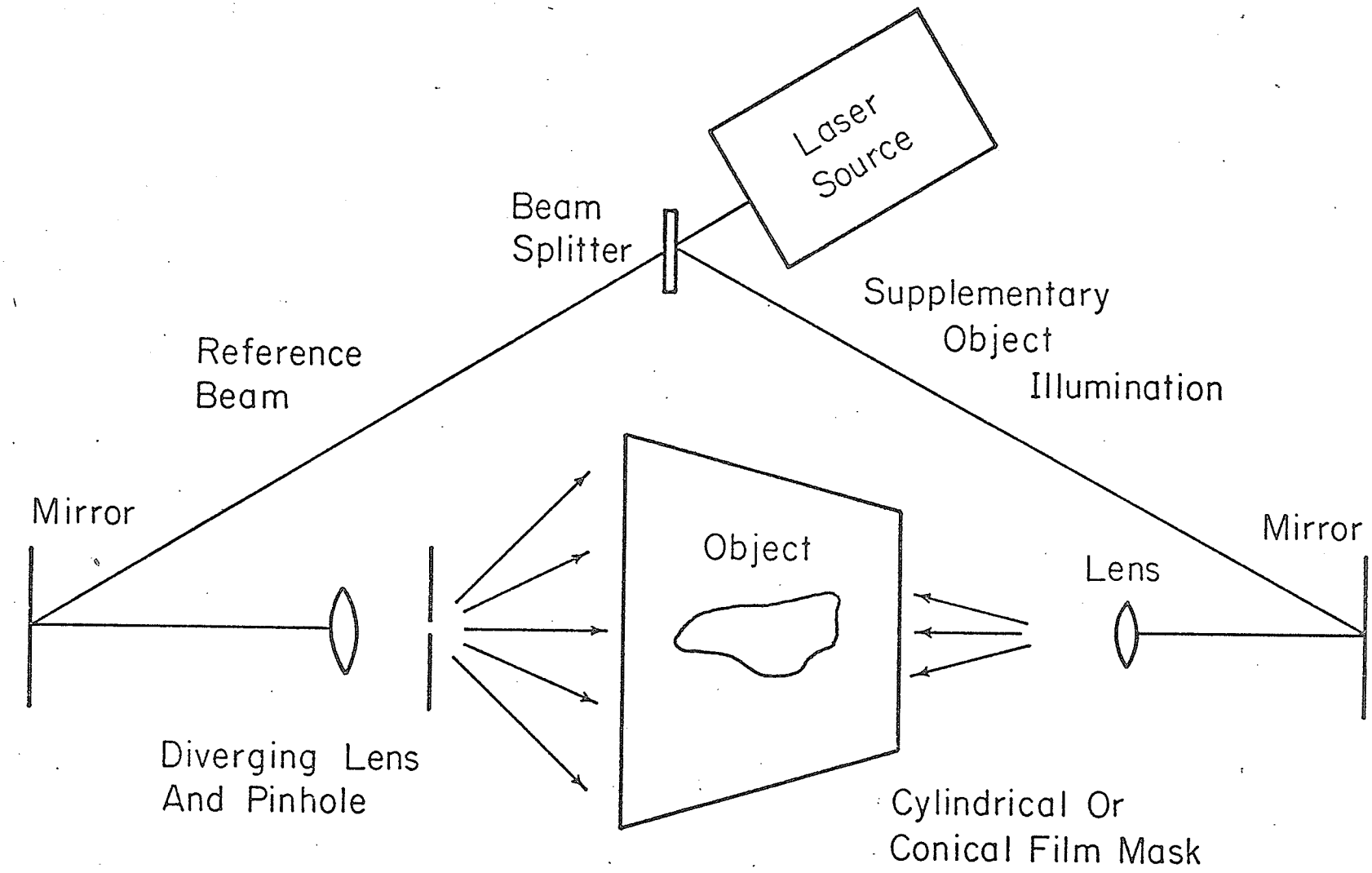

Fig. 4.2a Recording Geometry

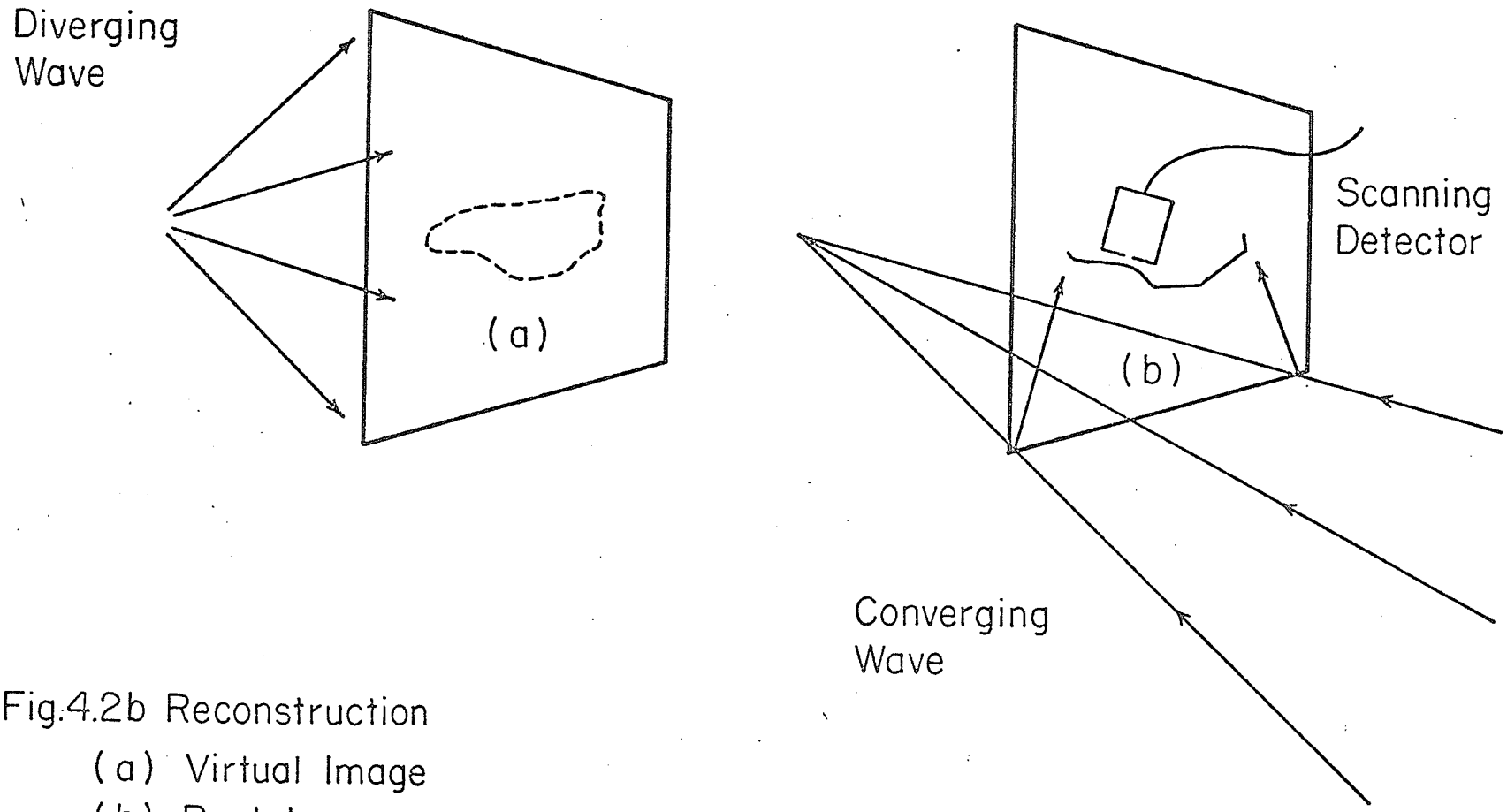

Fig.4.2b Reconstruction

(a) Virtual Image

(b) Real Image

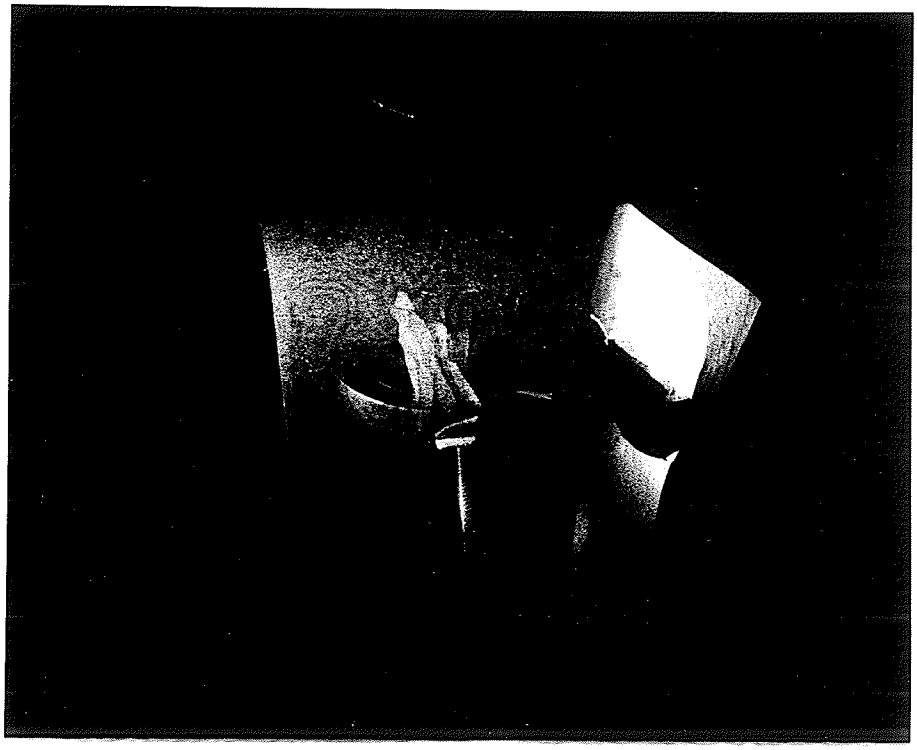

Photograph 4.9 Virtual image from cylindrical hologram

The hologram material is Agfa-Gavaert 10E75 flexible film and has not been bleached. The emulsion side of the film is facing inward. The reconstruction illumination duplicates the recording illumination and is a highly diverging spherical wave, incident from the left. The virtual image appearing through the film is of a small chess-piece (a knight). The dark bands referred to in the text, fringes of constant thickness [71], are readily apparent on the surface of the film. As commonly found in curvilinear holograms recorded on photographic film, the virtual image has less brightness, uniformity, contrast and resolution than similar planar holograms.

these holograms have less resolution, contrast and diffraction efficiency than those of planar holograms produced under more optimum conditions. Another prominent defect in these cylindrical holograms is the presence of brightand dark bands in the emulsion (see Photo 4.9) which tend to degrade the virtual image. These bright and dark bands are "fringes of constant thickness" [71] caused by multiple reflections of the reference wave in the film during recording. They can be reduced by the use of index matching solutions in a liquid gate.

chapter five

EXPERIMENTAL RESULTS

5.1 INTRODUCTION

The experiments of the preceding section were designed to test how well a holographic imaging system can approximate an ideal diffraction limited system when the recording medium is silver halide emulsion. Hopefully then, with this information, the performance of a curvilinear holographic imaging system can be predicted based on the theoretical analysis of *chapter three*.

No claim is made that the results obtained represent the optimum, however, they may be considered typical of a practical holographic system.

5.2 RESULTS OF EXPERIMENT 1

The intensity of the field near the focus of the real image of the point source was sampled with the aid of a flat film oriented perpendicular to the convergent axis. The point image as a function of distance from the focal point may be seen in Photographs 4.2, 4.3 and 4.4 and also in Fig. 5.1. From the figure it is obvious that the depth of focus is extremely limited. The focused image point (.18mm) is about 10 times the size of the original point but still represents very good resolution. From the photographs, it is apparent that the

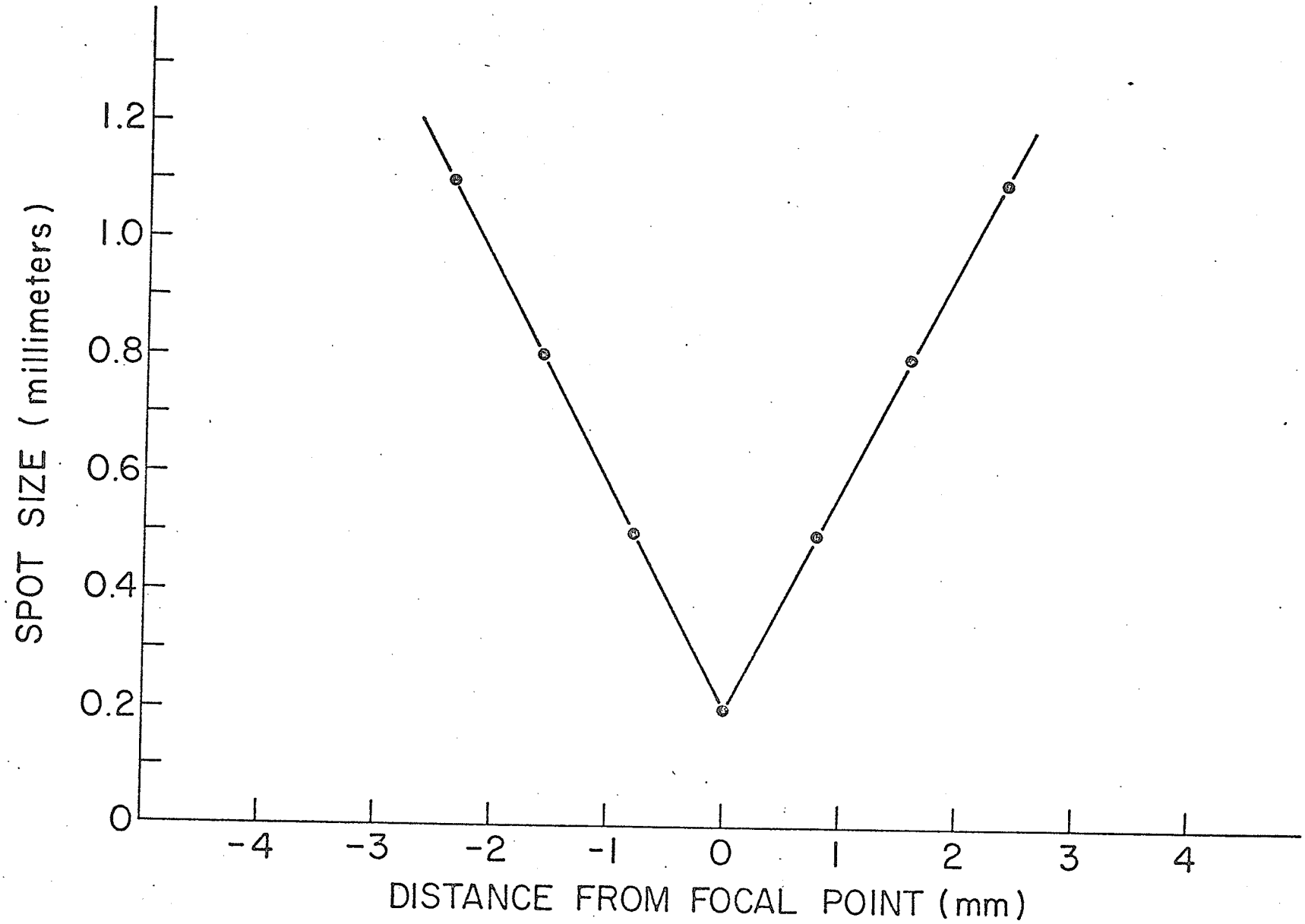

FIG. 5.1 REAL IMAGE SIZE ALONG CONVERGENT AXIS

amounts of astigmatism and coma aberration are extremely small. This indicates that the reconstruction beam was a very good approximation of the conjugate reference beam and shows the advantage of using a plane wave reference beam.

Some parameters for this experiment are as follows:

wavelength of illumination = 6328Å

effective aperture of hologram = 7.6 cm

average hologram-to-object-distance = 8 cm

equivalent "f-number" = 8/7.6 = 1.05

5.3 RESULTS OF EXPERIMENT 2

The real image field was sampled at different points along the convergent axis as in Exp. 1 and the results may be seen in Photographs 4.6, 4.7 and 4.8. The limited depth of focus is again very apparent.

It was desired to determine the resolution of the system as a function of the reciprocal f-number a/R, where a is the effective aperture of the hologram and R is the average hologram-to-object-distance. Some resolution of the real image is lost in recording the image on film. Therefore, in order to determine the resolution of the system, the real image was observed directly through a 10X microscope objective as the effective aperture was varied. The arrangement used to determine resolution is depicted in Fig. 5.2. The results may be seen in Fig. 5.3. Although the resolution obtained is much less than the ideal diffraction limited system, it is still very good.

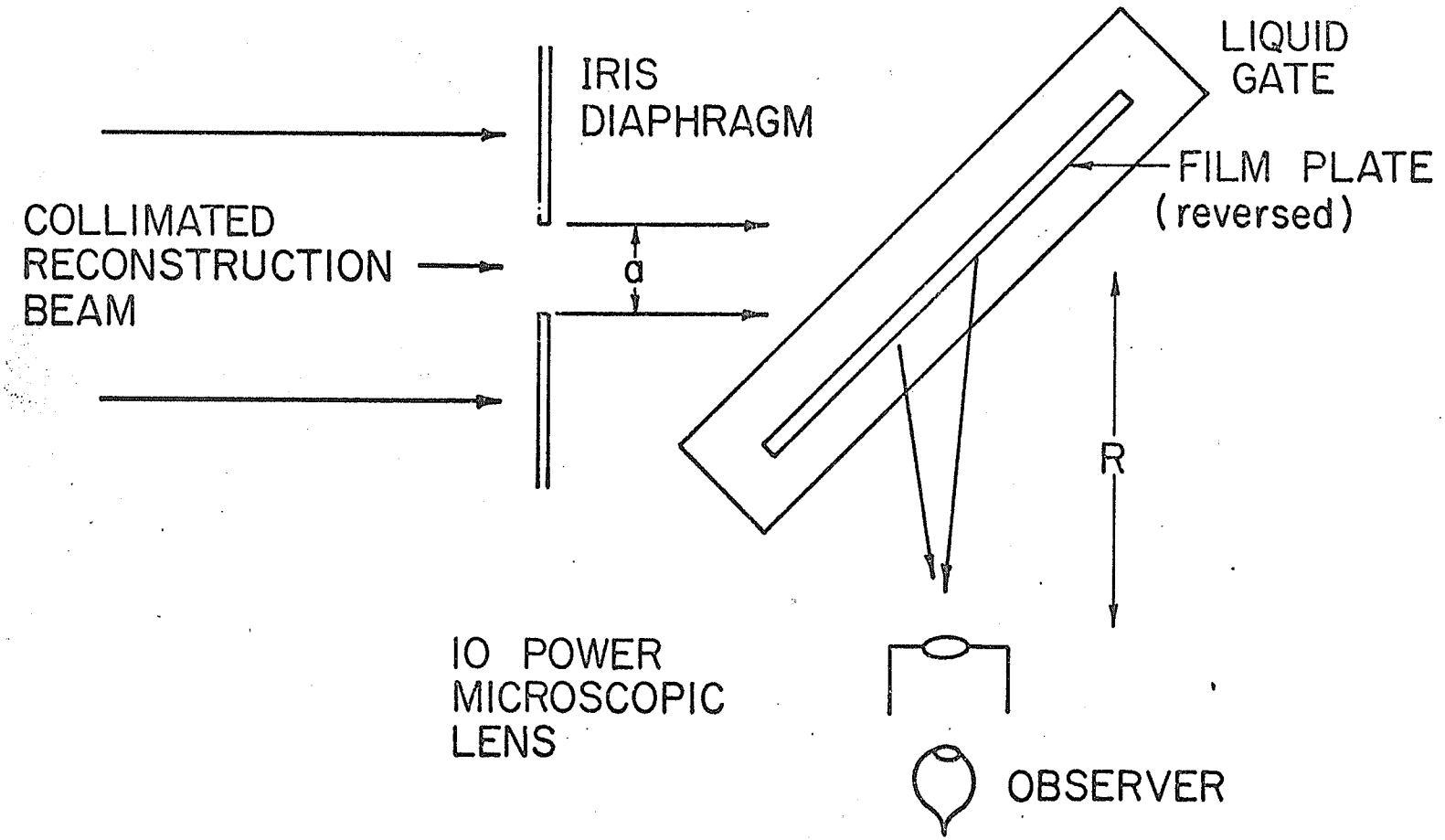

FIG. 5.2 DETERMINATION OF RESOLUTION AS A FUNCTION OF APERTURE a

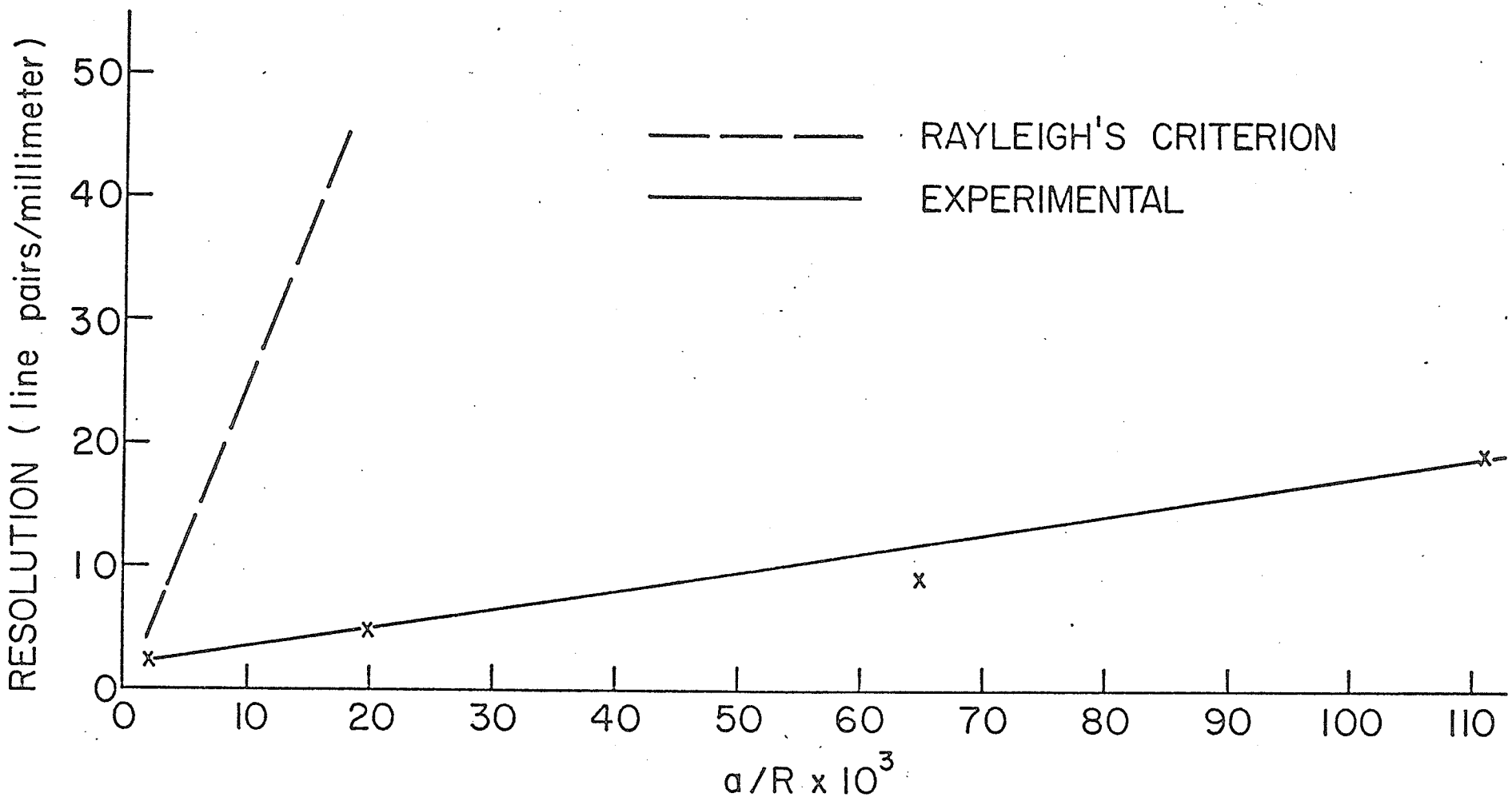

FIG. 5.3 PLOT OF IMAGE RESOLUTION AS A FUNCTION OF THE RECIPROCAL f-NUMBER (a/R)

5.4 RESULTS OF EXPERIMENT 3

A number of cylindrical and conical holograms have been made using the arrangement of Fig. 4.2. A typical virtual image can be seen in Photo. 4.9. In general, the virtual images produced by these holograms have less resolution, contrast and diffraction efficiency than those of planar holograms which can be made under more optimum conditions. The flexible nature of the film allows considerable distortion of the emulsion which results in a loss of object information. Any distortion of the emulsion causes serious information loss because the fringe frequency is very high, and the fringes lie, in general, at very oblique angles to the emulsion surface. Another prominent defect in these cylindrical holograms is the presence of bright and dark bands in the emulsion (see Photo. 4.9) which tend to degrade the virtual image. These bright and dark bands are "fringes of constant thickness" [71] caused by multiple reflections of the reference wave in the film during recording. These effects are caused by the very oblique angle at which the reference beam strikes the emulsion surface. Because of this, cylindrical holograms also exhibit more light scattering "noise".

Since suitable optics to form large-scale converging waves were not available, real images could not be formed from the available cylindrical holograms. The problem of obtaining suitable reconstruction beams for cylindrical holograms is a serious one. Large scale converging waves can be formed using large diameter lenses and parabolic mirrors. These optics have to be well corrected and are therefore quite expensive.

5.5 SUMMARY OF EXPERIMENTAL RESULTS

The results of EXPERIMENT 1 and EXPERIMENT 2 indicate that the resolution obtainable in the real image of a holographic system is more than sufficient for many practical engineering applications. The analysis of *chapter three* has shown the ideal resolution to be on the order of a wavelength of light. Therefore even though the experimentally obtainable resolution is only about 6.8% of that of the ideal system, (from Fig.5.3), it is still very high. The theoretical analysis of the ideal system can then be used to predict the performance of a real holographic system. The experiments have shown that good resolution can be obtained using silver halide recording materials provided precautions are taken to overcome the physical liabilities of the film and other components. It is suggested that cylindrical hologram real images can be made with equivalent resolution to that obtained in EXPERIMENT 1 and EXPERIMENT 2 if similar precautions are taken. Fig. 5.4 depicts a scheme which might make this possible. The arrangement of Fig.5.4 features a liquid gate to accomodate curvilinear holograms and a conical hologram shape to allow plane wave reference and reconstruction beams.

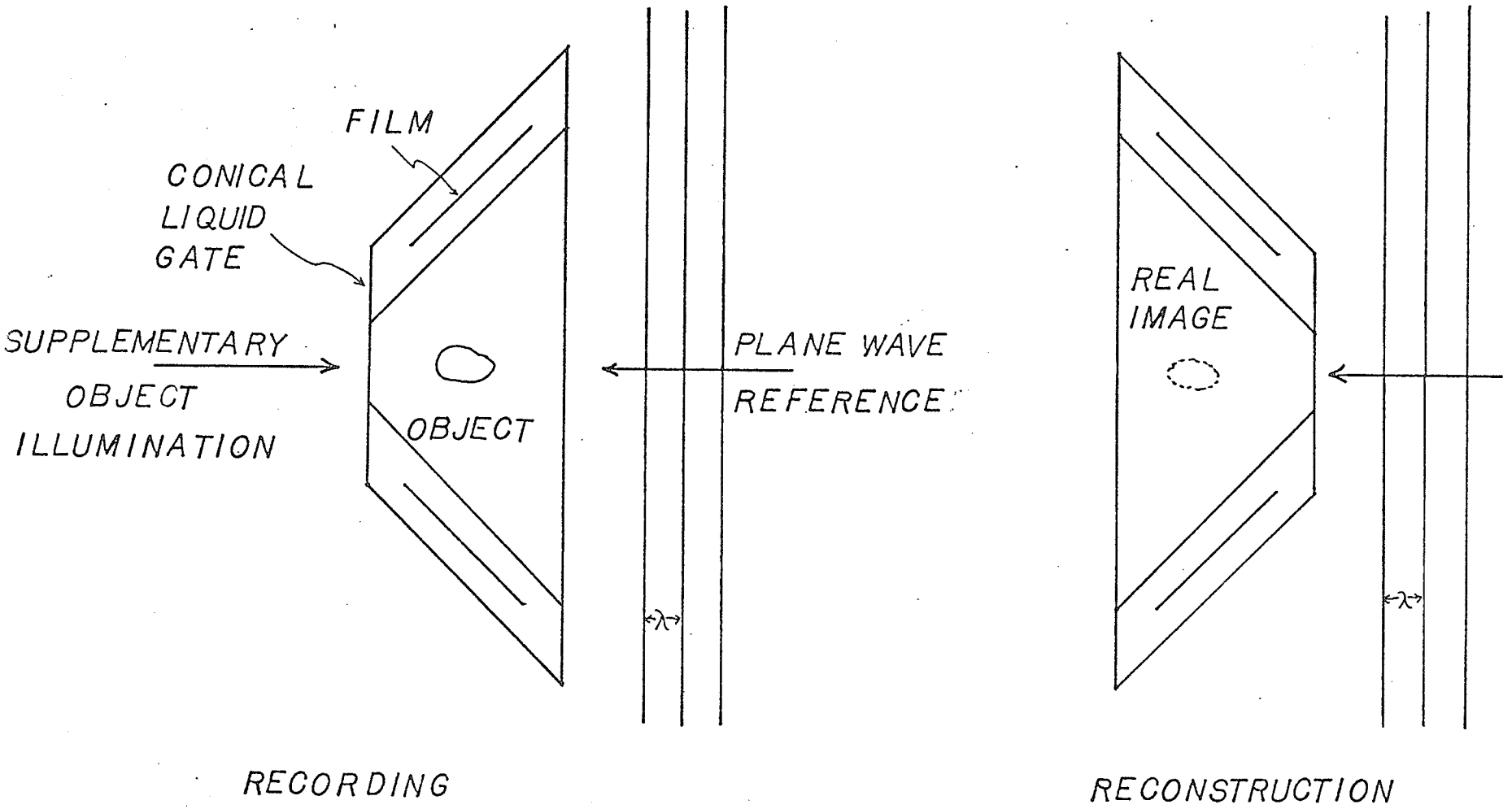

FIG. 5.4 PROPOSED CONICAL HOLOGRAM ARRANGEMENT

chapter six

CONCLUSIONS

This thesis has been concerned with aspects of real image generation by curvilinear holograms. The purpose was not to develop a rigorous theory of inverse scattering from curvilinear holograms, but rather to develop a model with which the performance of real systems can be predicted. The theory presented in *chapter three* has been developed with this objective in mind. Similarily, the experiments of *chapter four* were not designed to obtain the ultimate possible resolution of a holography system, but rather, they were designed to determine the resolution obtainable in a typical holography system when reasonable measures are used to overcome image degradation factors. Comparison of the results of *chapter four* with the theory of *chapter three* yields information upon which the performance of a practical holographic imaging system can be judged.

There havebeen tremendous developments in the field of holography since its inception in 1949. In the literature review of *chapter two*, a summary has been made of the pertinent contributions, both theoretical and practical, in the field of holographic imaging, with particular emphasis on curvilinear hologram shapes. As indicated in the summary, there are a great many factors which influence the quality of holographic images. These factors include the following: coherency of the interfering illumination [14], shifts in the interference pattern during recording due to vibration, air turbulence or heat gradients

[13,14], distortion of the recording media [13], inherent limitations of the recording media [20,61], nonlinearity of recordings [22,35], and the inability to exactly duplicate (or generate the conjugate of) a reference beam [20,63]. All these factors must be taken into consideration in the design of a holographic system.

Holograms have been conventionally analyzed assuming a planar hologram shape. Such models are clearly insufficient to determine the increase in resolution in large-angle curvilinear holograms. Some authors have considered imaging from large scale planar holograms [52][68][33] [10]. Porter [55] has shown that in two-dimensional curvilinear holograms, the resolution of the real image depends on subtended angle but not on aperture shape (when the hologram recording medium is ideal). *Chapter three* has presented a similar analysis for the case of the three-dimensional hologram.

Some authors have considered the possibility of object mensuration from holographic virtual images [45][50][51]. This method has been found [45] to involve very laborious procedures requiring highly complex instruments, subjective decision-making, and highly skilled personnel. It has been proposed that the mensuration system can be made much simpler, and perhaps automatic, if the real image is analyzed instead of the virtual image. Some success has been achieved with planar holograms [62][19]. The analysis of *chapter three* has indicated that curvilinear holograms, that surround a three-dimensional object during recording, contain enough information to reconstruct the scattering

surface with great detail. The resolution obtainable in the real image field was found to be directly proportional to the amount of object radiation that the hologram surface subtends.

In the experimental section, the theoretical resolution was compared with that of real holographic systems. According to Fig.5.3, the real system had a resolution corresponding to about 6.8% of the theoretical model. Since the resolution of the theoretical model is extreme (see *chapter three*), it can then be predicted that the resolution obtainable in curvilinear real imaging systems is sufficient to enable highly accurate mensuration of three-dimensional objects. Since the depth-of-focus [47] is proportional to the reciprocal of the resolution frequency of the system, the depth-of-focus of a curvilinear holographic system should be extremely small. This indicates that it should be possible to design equipment to sample the intensity of the real image field and thereby generate the contours of the scattering object with great accuracy. Gara and Majkowski [19] have been successful with a similar technique used with planar holograms. The increased resolution obtainable with curvilinear holograms should make the technique much more accurate. A convenient technique would be to use the end of a fiber optic as the sampling aperture. The resolution would then probably be on the order of the diameter of the fiber. The contours of the object could then be generated by computor from the sampled data. Other techniques such as recording the real image directly on film are also possible. EXPERIMENT 3 has shown that the images obtainable in conventional [26,27,28,29,64] cylindrical

holograms have much less resolution than that obtainable in planar holograms, in which the degrading effect of some physical phenomena can be avoided. Therefore it can be concluded that precautions analogous to those of EXPERIMENT 1 and EXPERIMENT 2 must be taken in order to obtain high-resolution cylindrical holograms. A possible method of achieving this is sketched in Fig.5.4. The arrangement features the use of a liquid gate and a conical hologram shape. The use of a conical hologram shape allows the use of a plane reference and reconstruction wave. This greatly simplifies the reconstruction geometry and ensures that the two beams are exactly the conjugates of one another thus effectively eliminating abberrations in the image. Note that the conjugate of a plane wave is simply another plane wave travelling in exactly the opposite direction.

It is proposed that a cylindrical holographic mensuration system can be used to obtain precise measurements on nonstationary objects if a pulsed laser is used instead of a continuous wave laser. The range of subjects would then include living tissue. Ansley [2] has shown that pulsed laser techniques can be used to obtain large-scale holograms of people. Special precautions must be taken [2][64] when the pulsed illumination is allowed to enter the eye. Such holograms require a laser source that is both powerful and has a long coherent length. Fortunately, as Dennis Gabor pointed out [73] in his Nobel Prize dissertation in 1971, "Nowadays single-mode pulses of 30 nano second duration with 10 joule in the beam and coherence lengths of 5-8 meters are available....". The upper bound on the size of cylin-

drical hologram subjects is determined by the coherent length of the laser source and by the availability of suitable optics and recording materials. The very short duration of the pulsed output of a pulsed laser imposes practically no restriction on the motion of the subject [2]. Thus the range of subjects suitable for cylindrical holography is extremely large and even includes living beings!

It has been demonstrated that curvilinear holography offers a workable technique for accurate mensuration of three-dimensional objects. It is obvious, however, that the technique can be useful in a virtually limitless number of applications. For example, cylindrical holograms can be used in information processing systems to obtain the cross-correlation or convolution of three-dimensional objects. Another possible application is the use of large scale curvilinear (spherical) holograms as diffraction lenses in astronomical telescopes. Such lenses would be much lighter in weight and much cheaper to produce than conventional lenses and would be particularly suited to use in outer space.

appendix A.1

EXPANSION OF GREEN'S FUNCTION [53][76]

The Green's function must satisfy the Sommerfeld radiation condition [71] and the differential equation

$$(\nabla^2 + k^2)G(\bar{r},\bar{r}') = -\delta(\bar{r} - \bar{r}') \quad , \qquad \text{(A-1)}$$

where $\bar{r}'$ denotes the source coordinates and $\bar{r}$ denotes the observation coordinates (Fig.3.1).

Equation (A-1) can be written [76] as a triple Fourier transform

$$\tilde{\tilde{G}}(\bar{\alpha},\bar{r}) = (2\pi)^{-3/2} \frac{\exp(-i\bar{\alpha}\cdot\bar{r}')}{\alpha^2 - k^2} \quad , \qquad \text{(A-2)}$$

the inverse of which is

$$G(\bar{r},\bar{r}') = (2\pi)^{-3} \iiint_{-\infty}^{\infty} \frac{\exp[i\bar{\alpha}\cdot(\bar{r}-\bar{r}')}{\alpha^2 - k^2} \, d\bar{\alpha} \quad . \qquad \text{(A-3)}$$

Using the change of variable

$$\tau = [k^2 - (\alpha_1^2 + \alpha_2^2)]^{1/2} \quad ;$$

then we can write Eqn.(A-3) as

$$G(\bar{r},\bar{r}') = (2\pi)^{-3} \iint_{-\infty}^{\infty} d\alpha_1 d\alpha_2 \exp\{i[\alpha_1(x-x') + \alpha_2(y-y')]\}$$
$$\times \int_{-\infty}^{\infty} \frac{\exp[i\alpha_3(Z-Z')]}{(\alpha_3+\tau)(\alpha_3-\tau)} \, d\alpha_3 \quad . \qquad \text{(A-4)}$$

The last integral on the right in Eqn.(A-4) can be evaluated by assuming α_3 to be complex and integrating about the contour of Fig.A-1, where the contribution along C_2 vanishes for $Z>Z'$ and the contribution along C_3 vanishes for $Z<Z'$. Thus we obtain

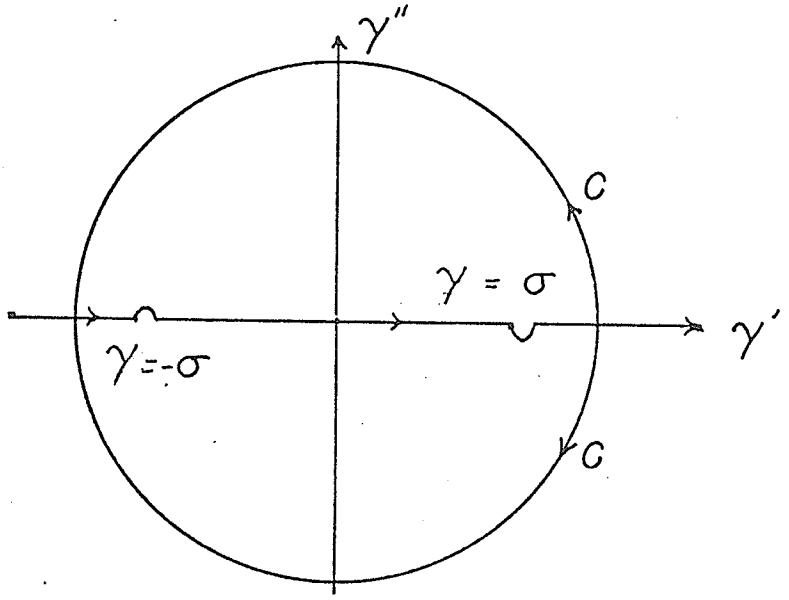

FIG. A-1 PATH OF INTEGRATION IN COMPLEX γ PLANE

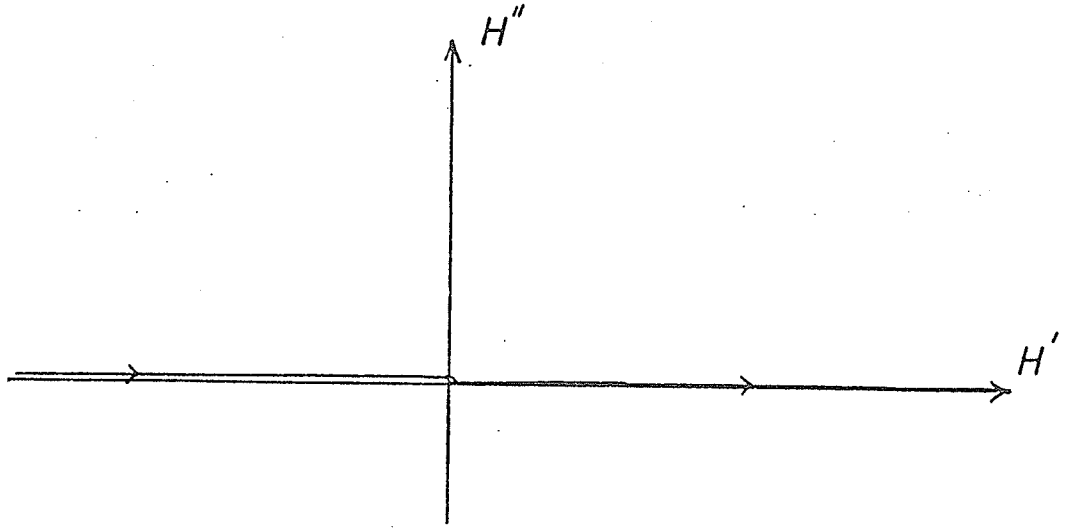

FIG. A-2 PATH OF INTEGRATION IN COMPLEX H PLANE
PATH CAN BE MODIFIED TO LIE ALONG REAL AXIS.

$$\int_{-\infty}^{\infty} \frac{\exp[i\alpha_3(Z-Z')]}{\alpha_3^2 - \tau^2}\, d\alpha_3 = \pi i \frac{\exp(i|Z-Z'|\tau)}{\tau} , \qquad (A-5)$$

which when substituted into Eqn.(A-4) gives

$$G(\bar{r},\bar{r}') = \frac{i}{8\pi^2} \iint_{-\infty}^{\infty} \tau^{-1}[\exp\{i[\alpha_1(x-x')+\alpha_2(y-y')+\tau|Z-Z'|]\}]d\alpha_1 d\alpha_2 . \qquad (A-6)$$

Now if we make the substitutions

$$\alpha_1 = \beta\cos\gamma \quad , \qquad x-x' = \rho\cos\phi \quad ,$$

$$\alpha_2 = \beta\sin\gamma \quad , \qquad y-y' = \rho\sin\phi \quad ,$$

we can then write Eqn.(A-6) in the form

$$G(\bar{r},\bar{r}') = \frac{i}{8\pi^2} \int_0^{\infty} (k^2-\beta^2)^{-1/2}\exp[i(k^2-\beta^2)^{1/2}|Z-Z'|]\beta d\beta$$

$$\times \int_{-\pi}^{\pi} \exp[ih\rho\cos(\gamma-\phi)]d\gamma . \qquad (A-7)$$

The last integral on the right can be identified as an integral representation of the Bessel function. Noting the formula

$$J_n(Z) = (2\pi)^{-1} \int_{-\pi}^{\pi} \exp[iZ\cos(\gamma-\phi) + in(\gamma-\phi-\pi/2)]d\gamma , \qquad (A-8)$$

where ϕ is an arbitrary angle we obtain

$$G(\bar{r},\bar{r}') = \frac{i}{4\pi} \int_0^{\infty} \frac{J_0(\beta\rho)\exp[i(k^2-\beta^2)^{1/2}|Z-Z'|\beta d\beta}{(k^2-\beta^2)^{1/2}} . \qquad (A-9)$$

The integral in Eqn.(A-9) can be reformulated into one running from $-\infty$ to ∞ by expressing the Bessel function in terms of Hankel functions. Using the change of variable, $h^2 = k^2-\beta^2$, we obtain

$$G(\bar{r},\bar{r}') = \frac{i}{8\pi} \int_{-\infty}^{\infty} H_o^{(1)}(\beta\rho)\exp[ih|Z-Z'|dh \quad , \qquad \text{(A-10)}$$

for the time dependance $\exp(-i\omega t)$ and

$$G(\bar{r},\bar{r}') = \frac{i}{8\pi} \int_{-\infty}^{\infty} H_o^{(2)}(\beta\rho)\exp[ih|Z-Z'|dh \quad , \qquad \text{(A-11)}$$

for the time dependance $\exp(i\omega t)$. The path of integration is shown in Fig.A-2.

appendix A.2

PHOTOGRAPHIC PROCESSING

INTRODUCTION

The interference fringes recorded in holograms are in general much finer than any image encountered in ordinary photography. In fact, the period of the fringes is usually much less than the thickness of the emulsion [61]. Because of this, holograms must be processed with considerably more care than ordinary photographs. The information capacity will be reduced or lost if any factor during processing causes the emulsion to be distorted by more than a small fraction of its thickness. Therefore, a careful processing schedule must be followed for obtaining optimal results. It is particularly important that all solutions be maintained at the same temperature to prevent random shifts in the emulsion [13].

Processing Procedure for Kodak and Agfa-Gevaert Holographic Films

The following basic processing procedure has been found to be effective:

1) Development: 5 min. in Kodak D-19 developer both with continuous agitation. Followed immediately by a 30 sec. rinse in Kodak indicator stop bath solution.
2) Fixation: 5 min. in Kodak Rapid Fixer bath with continuous agitation. Followed with a 30 sec. rinse in water.
3) Residual Fixer Removal: 2 min. in Kodak Hypo Clearing Agent bath.
4) Wash: 5 min. in flowing water.
5) Dry: Rinse in Kodak Photo-Flo solution and drip dry in air at

room temperature.

Note: All baths and wash waters should be maintained within one Celsius degree of the same temperature.

Drying Method

A drying method which can result in a more uniform emulsion thickness is the following: After Step (4), the wet emulsion is soaked in methyl alcohol for 2 min. with continuous agitation, and then in isopropyl alcohol for 1 min. The emulsion is then removed from the propanol bath and the excess propanol blown off immediately with a jet of dry air. This is to be done before the alcohol has a chance to evaporate and cause moisture from the air to condense on the emulsion.

Shrinkage Compensation

A difficulty often encountered in holography is the shrinkage of the emulsion (by about 15%) during the fixation stage of processing. In reflection holography [13], this is enough to shift the wavelength of reconstruction light from red light to green light. To overcome this difficulty a swelling stage can be introduced between Steps (4) and (5).

Swell: 15 min. in 5% triethanolamine $(CH_2OHCH_2)_3N$ solution.

Bleaching

A technique unique to holography consists of chemically bleaching the developed photographic film so that the information is stored as a variation of the refractive index of the emulsion rather than as an absorptive variation [37]. The effect of such bleaching has been found to be a great increase in diffraction efficiency at the expense of resolution and contrast [13].

Two effective bleaches are as follows:

1. Potassium Ferricyanide and Potassium Bromide Bleach

   Preparation: dissolve 7 grams of KBr and 8 grams of $K_3Fe(CN)_6$ in 1000 ml of distilled water.

   Procedure:

   a) Bleach for 5 min., agitate.

   b) Wash 15 min. in running water.

   c) Rinse in Photo-Flo.

2. R-10 Type Bleach

   Preparation:

   Stock Solution A:

   Distilled water - 500 ml.

   Ammonium bichromate - 20 grams.

   Concentrated sulfuric acid - 14 ml.

   Distilled water to make - 1000 ml.

   Stock Solution B:

   Potassium bromide - 92 grams.

   Distilled water to make - 1000 ml.

   Solution C:

   Kodak Hypo Clearing Agent bath.

   Solution D:

   Cupric Bromide ($CuBr_2$) - 5 grams.

   Photo-Flo with distilled water to make - 1000 ml.

   Procedure:

   a) Just before use, mix one part A and one part B to ten parts distilled water and use this as the bleaching solution.

b) Bleach and agitate for 1 min. after the plate has cleared - usually about 3-5 min.

c) Rinse in running water for a few seconds.

d) Soak and agitate for 1 min. in clearing bath, Solution C.

e) Rinse for 5 min. in running water.

f) Soak for 5 min. in Solution D.

The R-10 type bleach has been found to produce the highest diffraction efficiency [13,31]. However the Potassium Ferricyanide bleach is generally preferred because it is easier to use. Also, the R-10 bleach is susceptible to darkening under exposure to light whereas the Potassium Ferricyanide bleach is much more stable [66].

Conclusion

The methods and formulas listed above have been found effective with both Kodak 649F and Agfa-Gevaert 10E75 and 8E75 holographic films.

The bleaches described above have been found to greatly increase the efficiency of holograms at the expense of image resolution. The loss of resolution is due to distortion in the emulsion during the bleaching process.

Distortion in the drying stage and effects of surface roughness can be eliminated by immersing the film in a liquid gate before and after processing.

Further information and a relevant extensive list of references can be found in reference [13].

REFERENCES

1. Agfa-Gevaert Technical Information, Scientific Photography, Gevaert-Agfa N.V., Mortsel, July 1971.

2. Ansley, D.A., "Techniques for Pulsed Laser Holography of People", Appl. Opt. 9, 1970, p.815.

3. Bates, R.H. and Peters, T.M., "Towards Improvements in Tomography", New Zealand Journal of Science, 14, 1971, p.175.

4. Bragg, W.L., "An Optical Method of Representing the Results of X-Ray Analysis", Z. Kristallogr. Kristallgeometrie Kristallprys. Kristallchem., 70, 1929, p.475.

5. Bragg, W.L., "A New Type of 'X-Ray Microscope'," Nature, 143, 1939, p.678.

6. Brynghdahl, O. and Lohmann, A., "Nonlinear Effects in Holography", J. Opt. Soc. Amer., 58, 1968, p.1325.

7. Camatini, E., (Ed.), Optical and Acoustical Holography, Plenum Press, New York, 1972.

8. Caulfield, H.J. and Lu, S., The Application of Holography, Wiley, New York, 1970.

9. Cathey Jr., W.J., "Three-Dimensional Wavefront Reconstruction Using a Phase Hologram", J. Opt. Soc. Amer. 55, 1965, p.457.

10. Champagne, E.B., "Nonparaxial Imaging, Magnification and Aberration Properties in Holography", J.Opt. Soc. Amer. 57, 1967, p.51.

11. Chomat, M., "Diffraction Efficiency of Multiple-Exposure Thick Absorption Holograms", Optics Communications, 2, 1970, p.109.

12. Collier, R.J. and Pennington, K.S., "Multicolor Imaging from Holograms Formed on Two-Dimensional Media", Appl. Opt., 6, 1967, p.1091.

13. Collier, R.J., Burckhardt, C.B. and Lin, L.H., Optical Holography, Academic Press, New York, 1971.

14. DeVelis, J.B. and Reynolds, G.O., Theory and Applications of Holography, Addison-Wesley, Reading, Mass., 1967.

15. Frecska, S.A., "Characteristics of the Agfa-Gevaert Type 10E70 Holographic Film", Appl. Opt., 7, 1968, p.2312.

16. Friesen, A.A. and Belenka, J.S., "Effects of Film Nonlinearities in Holography", Appl. Opt., 6, 1967, p.1755.

17. Gabor, D., "A New Microscopic Principle", Nature, 161, 1948, p.777.

18. Gabor, D., "Microscopy by Reconstructed Wavefronts: II", Proc. of the Physical Soc., Sec. B, 64, 1951, p.303.

19. General Motors Research Laboratories, "Contour Holography", Search, 7, No.6, 1972, Technical Information Dept., General Motors Research Laboratories, Warren, Mich. 48090, U.S.A.

20. Goodman, J.W., Introduction to Fourier Optics, McGraw-Hill, New York, 1968.

21. Goodman, J.W., "Film-Grain Noise in Wavefront Reconstruction Imaging", J. Opt. Soc. Amer., 57, 1967, p.493.

22. Goodman, J.W. and Knight, G.R., "Effects of Film Nonlinearities on Wavefront Reconstruction Images of Diffuse Objects", J. Opt. Soc. Amer., 58, 1968, p.1276.

23. Hessel, K.R., "Use of Photochromic Glasses and Films in Optical Processing Applications", Sandia Laboratories Development Report SC-DR-71 0829, 1971.

24. Hildebrand, B.P. and Haines, K.A., "Multiple-Wavelength and Multiple-Source Holography Applied to Contour Generation", J. Opt. Soc. Amer., 57, 1967, p.155.

25. Hill, K.O. and Jull, G.W., "Holographic Noise Levels in Two Silver Halide Recording Media", Optica Acta, 18, 1971, p.729.

26. Hioki, R. and Suzuki, T., "Reconstruction of Wavefronts in All Directions", Japan J. Appl. Phys., 4, 1965, p.816.

27. Jeong, T.H., "Cylindrical Holography and Some Proposed Applications", J. Opt. Soc. Amer., 57, 1967, p.1396.

28. Jeong, T.H., Rudolf, P. and Luckett, A., "360° Holography", J. Opt. Soc. Amer., 56, 1966, p.1263.

29. Kakichoshrili, Sh. D., Kocaleva, A.I. and Rukhadze, V.A., "Circular Holography of Three-Dimensional Objects", Optics and Spectroscopy, 24, p.333.

30. Kalman, G., "Holography in Thick Media", Applications of Lasers to Photography and Information Handling, R.D. Murrey Ed., Soc. of Photo. Scientists and Engineers, 1968, p.99.

31. Kiemle, H. and Kreiner, W., "Lippmann-Bragg-Phasenhologramme Mit Hohem Wirkungsgrad", Physics Letters, 28A, 1968 , p.425.

32. King, M.C., "Multiple Exposure Hologram Recording of a Three-Dimensional Image with a 360° View", Appl. Opt. 7, 1968, p.1641.

33. Kozma, A. and Zelenka, J.S., "Effect of Film Resolution and Size in Holography", J. Opt. Soc. Amer., 1970, p.60, p.34.

34. Kozma, A., "Effects of Film-Grain Noise in Holography", J. Opt. Soc. Amer., 58, 1968 , p.436.

35. Kozma, A., Jull, G.W. and Hill, K.O., "An Analytical and Experimental Study of Nonlinearities in Hologram Recording", Appl. Opt. 9, 1970, p.721.

36. Lalor, E., "A New Approach to the Inverse Diffraction Problem", Proc. Phys. Soc. (London), Ser.2, 2, 1969, p.236.

37. Latta, J., "The Bleaching of Holographic Diffraction Grating for Maximum Efficiency", Appl. Opt., 7, 1968, p.2409.

38. Leith, E. and Upatnieks, J., "Reconstructed Wavefronts and Communication Theory", J. Opt. Soc. Amer., 52, 1962, p.1123.

39. Leith, E. and Upatnieks, J., "Wavefront Reconstruction with Continuous-Tone Objects", J. Opt. Soc. Amer., 53, 1963, p.1377.

40. Leith, E. and Upatnieks, J., "Wavefront Reconstruction with Diffused Illumination and Three-Dimensional Objects", J. Opt. Soc. Amer., 54, 1964, p.1295.

41. Leith, E., Kozma, A., Upatnieks, J., Marks, J. and Massey, N., "Holographic Data Storage in Three-Dimensional Media", Appl. Opt., 5, 1966, p.1303.

42. Lin, L.H., "Holographic Formation in Hardened Dichromated Gelatin Films", Appl. Opt., 8, 1969, p.963.

43, Lowenthal, S., Serres, J. and Arsenault, H., "Resolution and Film-Grain Noise in Fourier Transform Holograms Recorded with Coherent or Spatially Incoherent Light", Optics Communications, 1, 1970, p.438.

44. Maccowski, A., "Hologram Information Capacity", J. Opt. Soc. Amer. 60, 1970, p.21.

45. McDonnell, "Speckle in Holograms", Photogrammetric Engineering, 37, 1971, p.587.

46. Meier, R.W., "Optical Properties of Holographic Images", J. Opt. Soc. Amer., 57, 1967, p.895.

47. Meier, R.W., "Depth of Focus and Depth of Field in Holography", J. Opt. Soc. Amer., 55, 1965, p.1693.

48. Meier, R.W., "Magnification and Third-Order Aberrations in Holography", J. Opt. Soc. Amer., 55, 1965, p.987.

49. Mikaeliane, A.L., Axenchikiv, A.P., Bobrinev, V.I., Gulaniane, E., and Shatun, V., "Holograms on Photochromic Films", IEEE Quantum Electron., QE-4, 1968, p.757.

50. Mikhail, E., "Mensuration Aspects of Holograms", Photogrammetric Engineering, 37, 1971, p.267.

51. Mikhail, E., "Hologrammetric Mensuration and Mapping System", Photogrammetric Engineering, 37, 1971, p.447.

52. Mittra, R. and Ransom, P.L., Proceedings of the Symposium on Modern Optics, J. Fox, Ed., Polytechnic Press, Brooklyn, 1967, p.619.

53. Oberhettinger, F., "Diffraction of Waves by a Wedge", Comm. Pure and Appl. Math., 7, 1954, p.551.

54. Papoulis, A., Systems and Transforms with Applications in Optics, McGraw-Hill, New York, 1968.

55. Porter, R.P., "Diffraction-Limited, Scalar Image Formation with Holograms of Arbitrary Shape", J. Opt. Soc. Amer., 60, 1970, p.1051.

56. Rigden, J.D. and Gordon, E., "The Granularity of Scattered Optical Maser Light", Proc. IRE, 50, 1962, p.2367.

57. Russo, V. and Sottini, S., "Bleached Holograms", Appl. Opt., 7, 1968, p.202.

58. Shankoff, T.A., "Phase Holograms in Dichromated Gelatin", Appl. Opt., 7, 1968, p.2101.

59. Sherman, G.C., "Integral-Transform Formulation of Diffraction Theory", J. Opt. Soc. Amer., 57, 1962, p.1490.

60. Shewell, J.R. and Wolf, E., "Inverse Diffraction and a New Reciprocity Theorem", J. Opt. Soc. Amer., 58, 1968, p.1596.

61. Smith, H.M., Principles of Holography, Wiley-Interscience, New York, 1969.

62. Stetson, K.A., "Holographic Surface Contouring by Limited Depth of Focus", Appl. Opt., 7, 1968, p.987.

63. Stroke, G.W., An Introduction to Coherent Optics and Holography, Second Edition, Academic Press, New York, 1969.

64. Supertzi, E. and Rigler, A., "Wide-Angle Holography", J. Opt. Soc. Amer., 56, 1966, p.524.

65. Swope, C. and Koeste, C., "Eye Protection Against Lasers", Appl. Opt., 4, 1965, p.523.

66. Upatnieks, J. and Leonard, C., "Diffraction Efficiency of Bleached Photographically Recorded Interference Patterns", Appl. Opt., 8, 1969, p.85.

67. Urbach, J.C. and Meier, R.W., "Thermoplastic Xerographic Holography", Appl. Opt., 5, 1966, p.666.

68. Wolf, E., "Determination of the Amplitude and the Phase of Scattered Fields by Holography", J. Opt. Soc. Amer., 60, 1970, p.18.

69. Wolf, E. and Shewell, J., "The Inverse Wave Propagotor", Phys. Letters, 25A, 1967, p.417.

70. Young, M. and Kitteredge, F., "Amplitude and Phase Holograms Exposed on Agfa-Gevaert 10E75 Plates", Appl. Opt., 8, 1969, p.2353.

71. Born, M. and Wolf, E., Principles of Optics, Fourth Edition, Pergamon Press, Oxford, 1970.

72. Kodak Plates and Films for Science and Industry, Third Edition, Eastman Kodak Company, Rochester, New York, 1967.

73. Gabor, D., "Holography, 1948-1971", Proc.of the IEEE, 60, 1972, p.655.

74. Maue, A.W., "The Formulation of a General Diffraction Problem by Means of an Integral Equation", Z. Physik, 126, 1949, p.601.

75. Stratton, J.A., Electromagnetic Theory, McGraw-Hill, New York, 1941.

76. Tyras, G., Radiation and Propagation of Electromagnetic Waves, Academic Press, New York, 1969.